NASA TECHNICAL MEMORANDUM

NASA TM X-1115

NASA TM X-1115

FACILITY FORM 602
X65 17599 (ACCESSION NUMBER)
(THRU)
61 (PAGES)
2 (CODE)
(NASA CR OR TMX OR AD NUMBER)
01 (CATEGORY)

N72-73764
(NASA-TM-X-1115) AERODYNAMIC CHARACTERISTICS AT MACH NUMBERS 2.30, 2.60, AND 2.96 OF A SUPERSONIC TRANSPORT MODEL HAVING A FIXED, WARPED WING O.A. Morris, et al (NASA) Jul. 1965 61 p
Unclas
CC/99 33849
TO
By Authority of 10/27/71 Date 7/5/72

# AERODYNAMIC CHARACTERISTICS AT MACH NUMBERS 2.30, 2.60, AND 2.96 OF A SUPERSONIC TRANSPORT MODEL HAVING A FIXED, WARPED WING

*by Odell A. Morris and Roger H. Fourn*

*Langley Research Center*

*Langley Station, Hampton, Va.*

NATIONAL AERONAUTICS AND SPACE ADMINISTRATION • WASHINGTON, D. C. • JULY 1965

REPRODUCED BY
NATIONAL TECHNICAL
INFORMATION SERVICE
U. S. DEPARTMENT OF COMMERCE
SPRINGFIELD, VA. 22161

61

NASA TM X-1115

# AERODYNAMIC CHARACTERISTICS AT MACH NUMBERS 2.30, 2.60, AND 2.96 OF A SUPERSONIC TRANSPORT MODEL HAVING A FIXED, WARPED WING

By Odell A. Morris and Roger H. Fournier

Langley Research Center
Langley Station, Hampton, Va.

NOTICE

NATIONAL AERONAUTICS AND SPACE ADMINISTRATION

# AERODYNAMIC CHARACTERISTICS AT MACH NUMBERS 2.30, 2.60, AND 2.96 OF A SUPERSONIC TRANSPORT MODEL HAVING A FIXED, WARPED WING*

By Odell A. Morris and Roger H. Fournier
Langley Research Center

17599

## SUMMARY

An investigation has been conducted in the Langley Unitary Plan wind tunnel at Mach numbers of 2.30, 2.60, and 2.96 to determine the static longitudinal and lateral aerodynamic characteristics of a model of a fixed-wing supersonic transport configuration with a design Mach number of 2.60 (SCAT 15-F). The configuration had a 74° swept, warped wing with a reflexed trailing edge and four engine nacelles mounted below the reflexed portions of the wing. The investigation also included tests for a flat-wing model and for an unreflexed-warped-wing model with both a sharp wing leading edge and a rounded wing leading edge. All models had the same wing planform.

Results of the investigation showed that the maximum trimmed value of lift-drag ratio at the design Mach number of 2.60 and Reynolds number per foot of $3.0 \times 10^6$ was 7.9. Maximum values of trimmed lift-drag ratio varied from 8.2 at Mach number 2.30 to 7.4 at Mach number 2.96. The SCAT 15-F thus showed a significant improvement in performance over previously tested transport-type configurations. The complete configuration was longitudinally stable and indicated positive directional stability and positive effective dihedral for the angle-of-attack range tested. Results of tests for the flat-wing—body combination and the warped-wing—body combination showed that wing warp substantially increased the aerodynamic performance potential. Modification of the warped wing from a sharp-leading-edge wing to a rounded-leading-edge wing caused no performance penalty.

Author

## INTRODUCTION

The National Aeronautics and Space Administration has an intensive research program underway to provide the research background necessary to define and meet the design requirements for a commercially acceptable supersonic transport airplane. Results of some of the initial studies are reported in references 1 to 6.

In the investigation reported in reference 6, a configuration having variable-sweep auxiliary wing panels (SCAT 15-2.6) showed a significant improvement in performance over previously tested versions of the configuration. However, the feasibility studies in reference 7 indicated that the variable-sweep wing with the high-aspect-ratio, overlapping wing panels, as was used on the SCAT 15-2.6, would probably create severe structural design problems.

In a continuation of the transport study, some new design tools and technique, as well as essentially the same basic concepts used in the earlier SCAT 15 investigations, are applied to a design having a fixed wing. The resulting configuration (SCAT 15-F) has a highly swept, reflexed warped wing and a slender fuselage which is cambered to aline with the wing camber plane in the region of the fuselage. Four nacelles are located below the wing to simulate the engine installation. A vertical tail is located near each wing tip, and horizontal control surfaces are located along the wing trailing edges.

Tests of the complete configuration and various combinations of component parts were conducted over an angle-of-attack range at two angles of sideslip for Mach numbers 2.30, 2.60, and 2.96 at a Reynolds number per foot of $3.0 \times 10^6$. In order to determine the effects of wing warp and wing reflex, tests were also made for an unreflexed-warped-wing model and a flat-wing model. Results of the investigation, together with a limited analysis, are presented herein.

## DESIGN METHODS AND CONCEPTS

The SCAT 15-F configuration was designed to represent a long-range, 150-passenger supersonic transport airplane having a cruise Mach number near 2.60 and was intended to demonstrate the significantly greater aerodynamic potential available as the result of recent aerodynamic developments. The new aerodynamic technology consists of new concepts as well as important new design tools which permit analytic treatment of complex complete configurations through the use of the electronic computer.

In the interest of high performance potential, the following basic decisions were made at the outset of the present study:

(a) The wing should be warped to provide sufficient pitching moment at zero lift for self-trimming at the cruise point (the degree of warp is designated by a design lift coefficient of 0.08).

(b) The nacelles should be located beneath and rearward on the wing, which should be locally reflexed to fully exploit the beneficial lift-drag interference of the wing-nacelle combination.

(c) The vertical tails should be located near the wing tips in a region of high effectiveness in order to improve directional stability as well as to act as wing fences and reduce drag.

The analytic methods were then used to provide the design modifications necessary for the final definition of the complete configuration. Details of the methods upon which the electronic-computer programs were based may be found in references 8 to 10. The programs based on these methods permitted the calculation of configuration wave drag, wing warp, and both the flat-plate and warped-wing pressure distributions.

## SYMBOLS

The data in the present investigation are referred to the body-axis system (see fig. 1(a)) except for the lift and drag coefficients, which are referred to the stability-axis system. The moment reference center is located on the body axis 33.27 inches rearward of the nose of the model, a longitudinal station corresponding to 77 percent of the body length.

$A$ cross-sectional area, sq in.

$b$ reference wing span, 23.640 in.

$C_D$ drag coefficient, $\frac{\text{Drag}}{qS}$

$C_{D,b}$ nacelle base drag coefficient

$C_{D,c}$ balance-chamber drag coefficient

$C_{D,i}$ internal nacelle skin-friction drag coefficient

$C_L$ lift coefficient, $\frac{\text{Lift}}{qS}$

$C_{L_\alpha}$ lift-curve slope

$C_l$ rolling-moment coefficient, $\frac{\text{Rolling moment}}{qSb}$

$C_m$ pitching-moment coefficient, $\frac{\text{Pitching moment}}{qS\bar{c}}$

$C_{m,o}$ pitching-moment coefficient at zero lift

$C_n$ yawing-moment coefficient, $\frac{\text{Yawing moment}}{qSb}$

$C_Y$ side-force coefficient, $\frac{\text{Side force}}{qS}$

$\bar{c}$ mean aerodynamic chord of reference wing, 18.366 in.

| | |
|---|---|
| $d$ | diameter, in. |
| $L/D$ | lift-drag ratio |
| $M$ | free-stream Mach number |
| $q$ | free-stream dynamic pressure, lb/sq in. |
| $r$ | radius, in. |
| $S$ | reference wing area including fuselage intercept and outboard wing tips, 2.262 sq ft |
| $t$ | thickness of flat wing, in. |
| $x$ | longitudinal station, measured from model nose, in. |
| $x_w$ | distance from wing apex, measured in streamwise direction, in. |
| $y$ | spanwise distance, measured from wing center line, in. |
| $z_B$ | difference between body reference axis (see fig. 1(a)) and fuselage center line, positive when fuselage center line is above reference axis, in. |
| $z_u$ | upper surface ordinate in z-direction, measured from chord line, in. |
| $z_l$ | lower surface ordinate in z-direction, measured from chord line, in. |
| $\delta_e$ | free-stream deflection angle of wing trailing-edge control surfaces measured with respect to wing camber line |
| $V^{2/3}$ | total volume of wing, body, and nacelles minus area of nacelle stream tube |
| $\alpha$ | angle of attack, deg |
| $\beta$ | angle of sideslip, deg |
| $C_{l_\beta}$ | effective-dihedral parameter, $\frac{\partial C_l}{\partial \beta}$ at $\beta = 0^\circ$ |
| $C_{n_\beta}$ | directional-stability parameter, $\frac{\partial C_n}{\partial \beta}$ at $\beta = 0^\circ$ |
| $C_{Y_\beta}$ | side-force parameter, $\frac{\partial C_Y}{\partial \beta}$ at $\beta = 0^\circ$ |

$\frac{\partial C_m}{\partial C_L}$ longitudinal-stability parameter (or static margin, percent $\bar{c}$)

Subscripts:

max maximum

min minimum

Model component designations:

B body

E engine nacelle

V vertical tail

W warped wing with unreflexed trailing edge and sharp leading edge

$W_F$ flat wing

$W_M$ unreflexed warped wing modified with rounded wing leading edge

$W_R$ warped wing with reflexed trailing edge

## MODEL AND APPARATUS

Details of the complete model configuration, which incorporated the warped wing with the reflexed trailing edge, are shown in figure 1 and table I. The 74° swept wing of arrow-wing planform had a subsonic leading edge except in the region of the tip where the leading-edge sweep was decreased to 65°. The wing trailing-edge sweep of 45° provided a sizable trailing-edge cutout which reduced the inefficient lifting surface in the region of the wing trailing edge. The wing trailing edge was reflexed upward from about 1.25° to 2.68° in the region of the flow field from the engine nacelles, as shown in figure 1(b), in order to essentially cancel the lift interference from the nacelles (and an attendant negative moment increment) and to improve the drag interference effects of the wing-nacelles combination. The juncture between the reflexed section of the wing and the remaining wing surface was faired smooth so that no sharp break existed on the wing in this region. The vertical tails were mounted on the outboard wing panels in order to improve the directional stability and also to improve flow in the wing-tip region by providing a "fencing" effect which had been noted in previous tests of a warped-arrow-wing configuration (ref. 11). The tails were also canted outward 1.6° in order to aline them with the local flow at the design lift coefficient and to reduce the drag increment due to the tails. The model was constructed so that various combinations of the component parts could be investigated, and the wing was equipped with movable trailing-edge controls, as shown in figure 1(e), to provide for control deflection tests.

Two other models, a warped-wing—body combination and a flat-wing—body combination, were also investigated. The warped-wing model was identical in wing-body combination to the complete configuration except that the wing was unreflexed along the trailing edge. Low-speed tests indicated that a rounded wing leading edge would be desirable for the low-speed range so tests were also conducted on the unreflexed-warped-wing model with the original sharp leading edge of the wing modified to a rounded leading edge. The modification was made by gluing two narrow wood strips along the upper and lower surfaces of the wing leading edge, which tapered linearly in thickness from the wing root to the outboard wing station where the vertical tails were located. The region rearward of the strips (shown in fig. 2) was filled and faired smooth and the wing leading edge was rounded to a radius approximately equal to the local thickness of the strips. The flat-wing—body model had the same wing planform and normal cross-sectional area as the other two models, but had an unwarped wing and a straight body mounted symmetrically about the wing center line. (See fig. 3.)

Wing and body coordinates for each model are given in tables II and III, respectively. The normal cross-sectional area for some of the models and component parts is presented in figure 4. The normal area distribution would be identical for all three wing-body combinations. The models were mounted in the tunnel on a remote-controlled sting, and force measurements were made through the use of a six-component internal strain-gage balance. A photograph of the complete configuration is shown in figure 5.

## TESTS, CORRECTIONS, AND ACCURACY

The investigation was conducted in the Langley Unitary Plan wind tunnel to determine the static longitudinal and lateral aerodynamic characteristics of the complete configuration. Tests were made through an angle-of-attack range of about $-10^\circ$ to $7^\circ$ at angles of sideslip of $0^\circ$ and $3^\circ$ for Mach numbers of 2.30, 2.60, and 2.96. The stagnation temperature was constant at $150^\circ$ F, and the Reynolds number per foot was constant at $3.0 \times 10^6$. Other test conditions are summarized in the following table:

| Mach number | Stagnation pressure, lb/sq ft |
|---|---|
| 2.30 | 2292 |
| 2.60 | 2679 |
| 2.96 | 3247 |

The angles of attack and sideslip were corrected for the deflection of the balance and sting under aerodynamic load and for tunnel flow angularity. The balance-chamber pressure and nacelle base pressure were measured, and the drag force was adjusted to a base pressure equal to free-stream static pressure. In addition, the drag results have been corrected for the internal skin-friction drag of the nacelles as well as the drag component of the normal force

associated with turning the air passing through the nacelles from the free-stream to the nacelle-axis direction. The magnitude of the internal skin-friction drag of the nacelles, the model chamber drag correction, and the nacelle base drag coefficients are shown in figure 6.

In order to assure a turbulent-boundary-layer condition, 1/16-inch-wide transition strips of No. 60 carborundum grit were applied 1/2 inch from the nose of the body and 1/2 inch (measured streamwise) from the leading edges of the wing and vertical tails. Transition strips were also located 1/2 inch from the inlets on both the outer and inner surfaces of the engine nacelles with No. 60 grit on the outer surface and No. 80 grit on the inner surface.

The estimated accuracy of the individual measured quantities is as follows:

| | |
|---|---|
| $C_L$ | ±0.0020 |
| $C_D$ | ±0.0002 |
| $C_m$ | ±0.0003 |
| $C_l$ | ±0.0001 |
| $C_n$ | ±0.0002 |
| $C_Y$ | ±0.0004 |
| $\alpha$, deg | ±0.10 |
| $\beta$, deg | ±0.10 |

## PRESENTATION OF RESULTS

The results of the investigation are presented in the following figures:

## DISCUSSION

### Longitudinal Aerodynamic Characteristics

A comparison of the longitudinal aerodynamic characteristics for the three wing-body models is shown in figure 7. Both the reflexed- and unreflexed-warped-wing models had larger values of $(L/D)_{max}$ than did the flat-wing model. However, this improvement in $(L/D)_{max}$ decreased with increasing Mach number so that at $M = 2.96$ the improvement due to wing warp was relatively small. Large favorable increases in positive values of $C_m$ were obtained at zero lift for both warped-wing models, with the higher values occurring for the reflexed-warped-wing model, as might be expected. The positive values of $C_{m,o}$ obtained for the warped-wing models tend to produce good self-trimming characteristics with little or no control deflection required at the design cruise lift coefficient. Thus, by providing large positive pitching moments at zero lift, wing warp contributed significantly toward the attainment of high maximum trimmed values of L/D.

The data in figures 8 and 9 show that addition of the vertical tails to both the unreflexed-warped-wing model and the reflexed-warped-wing model produced only small adverse changes in the measured longitudinal characteristics. Also a comparison of the data in figure 8 for the sharp-leading-edge wing and the modified rounded-leading-edge wing showed no performance penalty due to blunting in the Mach number range of the investigation. Since leading-edge blunting would be likely to improve low-speed aerodynamic characteristics, such a modification would appear to be desirable.

Addition of the engine nacelles on the reflexed-warped-wing combination (fig. 9) caused an increase in the minimum drag and also an increase in lift due to the favorable interference effects of the nacelles on the wing so that only a slight decrease occurred in the maximum values of L/D. Note that, as anticipated, lift curves for the reflexed-warped-wing configuration with nacelles (fig. 9) closely approximate those for the unreflexed-warped-wing configuration without nacelles (fig. 8). A comparison of the corresponding sets of pitching-moment curves shows the trim points to be somewhat different. However, the reflexed configuration with nacelles is self-trimmed at the maximum lift-drag ratio.

The importance of self-trimming characteristics may be noted in the control-deflection data shown in figure 10. For a $6^\circ$ negative deflection of the wing-trailing-edge control surfaces, a reduction in the value of $(L/D)_{max}$ of about 8 percent occurred at $M = 2.60$ with similar reduction shown at the two other Mach numbers. For a positive control deflection of $7.5^\circ$, no large reductions in $(L/D)_{max}$ occurred since the controls were deflected downward so that the wing lift was increased. However, at the higher positive control deflection of $15^\circ$, a large reduction in $(L/D)_{max}$ occurred due to a sizable increase in drag which overshadowed the favorable increase in lift. The pitching-moment effectiveness of the controls was relatively low, due to the short moment arm and small area of the control surfaces.

The longitudinal parameters of the SCAT 15-F configuration are compared in figure 11 with results for two previously tested SCAT 15 models. At each Mach number, the SCAT 15-F has lower minimum drag values and significantly higher maximum values of trimmed lift-drag ratio. The maximum trimmed values of lift-drag ratio for the complete configuration varied from about 8.2 at Mach number 2.30 to about 7.4 at Mach number 2.96 at the test Reynolds number per foot of $3.0 \times 10^6$. At the design Mach number of 2.60, the maximum value of trimmed lift-drag ratio was 7.9. A significantly lower stability level was set for the present configuration because, in contrast to the two previous configurations with variable-sweep wing panels, the SCAT 15-F required no provision for stability change due to sweep.

## Lateral Aerodynamic Characteristics

The variations of the sideslip derivatives with angle of attack for the reflexed-warped-wing configuration are presented in figure 12. A stabilizing increment in $C_{n_\beta}$ was provided by the vertical tails and showed only a small variation with angle of attack. Addition of the engine nacelles also provided a positive increment in $C_{n_\beta}$ so that the complete model configuration had a positive level of directional stability that was essentially invariant over the test angle-of-attack range. The variation of $C_{l_\beta}$ with angle of attack for the complete model was fairly linear and indicated a positive dihedral effect which tended to increase with increasing angle of attack.

The variation of the sideslip derivatives with angle of attack for the unreflexed-warped-wing configuration is shown in figure 13. Comparison of the sideslip derivatives for the unreflexed- and reflexed-wing models showed that wing reflex had no significant effect on the lateral aerodynamic characteristics.

## CONCLUSIONS

An investigation has been made in the Langley Unitary Plan wind tunnel at Mach numbers of 2.30, 2.60, and 2.96 to determine the static longitudinal and lateral aerodynamic characteristics of a model of a fixed-wing supersonic transport configuration with a design Mach number of 2.60 (SCAT 15-F). The configuration had a $74^\circ$ swept, warped wing with a reflexed trailing edge and four engine nacelles mounted below the reflexed portions of the wing. The investigation also included tests for a flat-wing model and for an unreflexed-warped-wing model with both a sharp wing leading edge and a rounded wing leading edge. All models had the same wing planform. The following results were indicated:

1. The maximum trimmed values of lift-drag ratio for the complete configuration varied from about 8.2 at a Mach number of 2.30 to about 7.4 at a Mach number of 2.96 at the test Reynolds number per foot of $3.0 \times 10^6$. At the design Mach number of 2.60, the maximum value of trimmed lift-drag ratio was 7.9. The SCAT 15-F thus showed a significant improvement in performance over any previously tested transport configuration.

2. Results of tests for the flat-wing and the warped-wing models indicated that wing warp contributed significantly toward the attainment of high maximum trimmed values of lift-drag ratio.

3. Modification of the warped wing from a sharp-leading-edge wing to a rounded-leading-edge wing caused no performance penalty.

4. The complete configuration was longitudinally stable and indicated positive levels of directional stability and a positive effective dihedral for the test angle-of-attack range.

Langley Research Center,
National Aeronautics and Space Administration,
Langley Station, Hampton, Va., March 26, 1965.

## REFERENCES


1. Whitcomb, Richard T.; Patterson, James C., Jr.; and Kelly, Thomas C.: An Investigation of the Subsonic, Transonic, and Supersonic Aerodynamic Characteristics of a Proposed Arrow-Wing Transport Airplane Configuration. NASA TM X-800, 1963.

2. Driver, Cornelius; Spearman, M. Leroy; and Corlett, William A.: Aerodynamic Characteristics at Mach Numbers From 1.61 to 2.86 of a Supersonic Transport Model With a Blended Wing-Body, Variable-Sweep Auxiliary Wing Panels, Outboard Tail Surfaces, and a Design Mach Number of 2.2. NASA TM X-817, 1963.

3. Morris, Odell A.; and Fuller, Dennis E.: Aerodynamic Characteristics of a Three-Engine Supersonic Transport Model Having a Low-Aspect-Ratio Variable-Sweep Warped Wing. NASA TM X-1011, 1964.

4. Spearman, M. Leroy; Driver, Cornelius; and Robins, A. Warner: Aerodynamic Characteristics at Mach Numbers of 2.30, 2.96, and 3.50 of a Supersonic Transport Model With a Blended Wing-Body, Variable-Sweep Auxiliary Wing Panels, and Outboard Tail Surfaces. NASA TM X-803, 1963.

5. Henderson, William P.: A Low-Speed Longitudinal Stability Improvement Study on a Highly Swept Supersonic Transport Configuration. NASA TM X-1071, 1965.

6. Robins, A. Warner; Spearman, M. Leroy; and Harris, Roy V., Jr.: Aerodynamic Characteristics at Mach Numbers of 2.30, 2.60, and 2.96 of a Supersonic Transport Model With a Blended Wing-Body, Variable-Sweep Auxiliary Wing Panels, Outboard Tail Surfaces, and a Design Mach Number of 2.6. NASA TM X-815, 1963.

7. Proceedings of NASA Conference on Supersonic-Transport Feasibility Studies and Supporting Research. NASA TM X-905, 1963.

8. Harris, Roy V., Jr.: An Analysis and Correlation of Aircraft Wave Drag. NASA TM X-947, 1964.

9. Carlson, Harry W.; and Middleton, Wilbur D.: A Numerical Method for the Design of Camber Surfaces of Supersonic Wings With Arbitrary Planforms. NASA TN D-2341, 1964.

10. Middleton, Wilbur D.; and Carlson, Harry W.: A Numerical Method for Calculating the Flat-Plate Pressure Distributions on Supersonic Wings of Arbitrary Planform. NASA TN D-2570, 1965.

11. Morris, Odell A.; and Robins, A. Warner: Aerodynamic Characteristics at Mach Number 2.01 of an Airplane Configuration Having a Cambered and Twisted Arrow Wing Designed for a Mach Number of 3.0. NASA TM X-115, 1959.

TABLE I.- GEOMETRIC CHARACTERISTICS OF MODEL

| | |
|---|---|
| **Wing:** | |
| Aspect ratio | 1.717 |
| Span, in. | 23.640 |
| Area, sq ft | 2.262 |
| Root chord, at fuselage center line, in. | 28.264 |
| Tip chord, in. | 1.407 |
| Mean aerodynamic chord, in. | 18.366 |
| Thickness-chord ratio, root | 0.0321 |
| Thickness-chord ratio, tip | 0.0275 |
| Wetted area, sq ft | 3.9744 |
| **Fuselage:** | |
| Length, in. | 43.255 |
| Balance-chamber area, sq ft | 0.01227 |
| Wetted area, sq ft | 1.41670 |
| **Vertical tails:** | |
| Area (each), sq ft | 0.0777 |
| Airfoil section | Half circular arc |
| Thickness-chord ratio | 0.02 |
| Total wetted area (both), sq ft | 0.30960 |
| **Nacelles:** | |
| Length, in. | 7.500 |
| Capture area (each), sq ft | 0.00489 |
| Base area (each), sq ft | 0.00509 |
| Total wetted area (4 nacelles), sq ft | 0.80520 |
| $\frac{V^{2/3}}{S}$ | 0.10625 |

TABLE II.- WING COORDINATES

[All dimensions in inches]

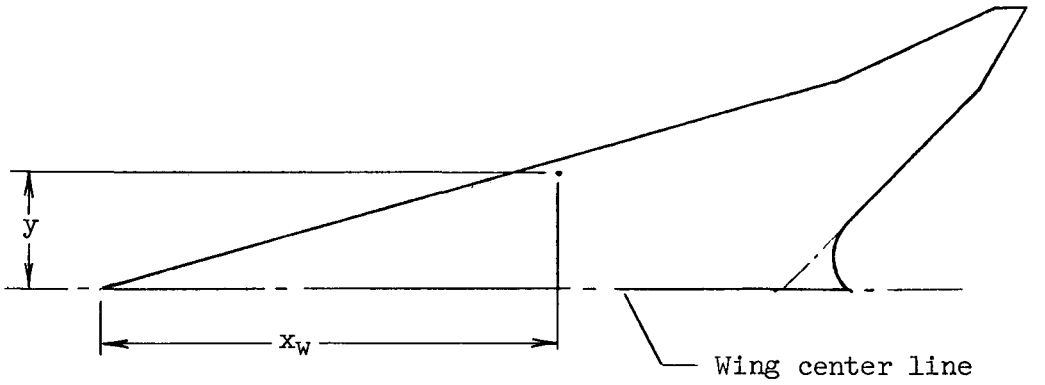


| $x_w$ | Unreflexed warped wing | | Reflexed warped wing | | Flat wing |
|---|---|---|---|---|---|
| | $z_u$ | $z_l$ | $z_u$ | $z_l$ | t/2 |
| y = 0.5911 | | | | | |
| 2.0612 | 1.9250 | 1.9250 | 1.9250 | 1.9250 | 0 |
| 2.8080 | 1.9440 | 1.8426 | 1.9440 | 1.8426 | .0507 |
| 3.5548 | 1.9431 | 1.7445 | 1.9431 | 1.7445 | .0993 |
| 4.3016 | 1.9269 | 1.6349 | 1.9269 | 1.6349 | .1460 |
| 5.0484 | 1.9002 | 1.5200 | 1.9002 | 1.5200 | .1902 |
| 6.5420 | 1.8228 | 1.2786 | 1.8228 | 1.2786 | .2721 |
| 8.0356 | 1.7222 | 1.0320 | 1.7222 | 1.0320 | .3451 |
| 9.5292 | 1.6039 | .7859 | 1.6039 | .7859 | .4090 |
| 11.0227 | 1.4739 | .5431 | 1.4739 | .5431 | .4654 |
| 14.0099 | 1.1851 | .0849 | 1.1851 | .0849 | .5505 |
| 16.9971 | .8746 | -.3272 | .8746 | -.3272 | .6009 |
| 19.9843 | .5530 | -.6796 | .5530 | -.6796 | .6163 |
| 22.9715 | .2077 | -.9417 | .2077 | -.9417 | .5747 |
| 25.9586 | -.1724 | -1.0884 | -.1724 | -1.0884 | .4580 |
| 28.9458 | -.5816 | -1.1144 | -.5816 | -1.1144 | .2664 |
| 31.9330 | -1.0146 | -1.0146 | -.940 | -.940 | 0 |

TABLE II.- WING COORDINATES - Continued

| $x_w$ | Unreflexed warped wing | | Reflexed warped wing | | Flat wing |
|---|---|---|---|---|---|
| | $z_u$ | $z_l$ | $z_u$ | $z_l$ | t/2 |
| y = 0.8866 | | | | | |
| 3.0919 | 1.5950 | 1.5950 | 1.5950 | 1.5950 | 0 |
| 3.8058 | 1.6099 | 1.5399 | 1.6099 | 1.5399 | .0350 |
| 4.5197 | 1.6211 | 1.4835 | 1.6211 | 1.4835 | .0688 |
| 5.2337 | 1.6076 | 1.4054 | 1.6076 | 1.4054 | .1011 |
| 5.9476 | 1.5857 | 1.3225 | 1.5857 | 1.3225 | .1316 |
| 7.3754 | 1.5205 | 1.1439 | 1.5205 | 1.1439 | .1883 |
| 8.8033 | 1.4346 | .9568 | 1.4346 | .9568 | .2389 |
| 10.2311 | 1.3320 | .7658 | 1.3320 | .7658 | .2831 |
| 11.6589 | 1.2184 | .5756 | 1.2184 | .5756 | .3214 |
| 14.5146 | .9659 | .2063 | .9659 | .2063 | .3798 |
| 17.3703 | .6923 | -.1351 | .6923 | -.1351 | .4137 |
| 20.2260 | .4086 | -.4374 | .4086 | -.4374 | .4230 |
| 23.0817 | .1069 | -.6781 | .1069 | -.6781 | .3925 |
| 25.9373 | -.2166 | -.8407 | -.2166 | -.8407 | .3118 |
| 28.7930 | -.5566 | -.9186 | -.5566 | -.9186 | .1810 |
| 31.6487 | -.9091 | -.9091 | -.860 | -.860 | 0 |
| y = 1.1821 | | | | | |
| 4.1224 | 1.2250 | 1.2250 | 1.2250 | 1.2250 | 0 |
| 4.8058 | 1.2464 | 1.1774 | 1.2464 | 1.1774 | .0330 |
| 5.4891 | 1.2776 | 1.1482 | 1.2776 | 1.1482 | .0647 |
| 6.1724 | 1.2774 | 1.0872 | 1.2774 | 1.0872 | .0951 |
| 6.8558 | 1.2747 | 1.0271 | 1.2747 | 1.0271 | .1238 |
| 8.2225 | 1.2421 | .8881 | 1.2421 | .8881 | .1770 |
| 9.5893 | 1.1898 | .7410 | 1.1898 | .7410 | .2244 |
| 10.9559 | 1.1216 | .5900 | 1.1216 | .5900 | .2658 |
| 12.3227 | 1.0407 | .4371 | 1.0407 | .4371 | .3018 |
| 15.0561 | .8492 | .1378 | .8492 | .1378 | .3557 |
| 17.7896 | .6308 | -.1426 | .6308 | -.1426 | .3867 |
| 20.5230 | .3933 | -.3947 | .3933 | -.3947 | .3940 |
| 23.2564 | .1303 | -.5967 | .1303 | -.5967 | .3635 |
| 25.9898 | -.1607 | -.7359 | -.1607 | -.7359 | .2876 |
| 28.7233 | -.4750 | -.8087 | -.4736 | -.8064 | .1664 |
| 31.4567 | -.8084 | -.8084 | -.742 | -.742 | 0 |

TABLE II.- WING COORDINATES - Continued

| $x_w$ | Unreflexed warped wing | | Reflexed warped wing | | Flat wing |
|---|---|---|---|---|---|
| | $z_u$ | $z_l$ | $z_u$ | $z_l$ | t/2 |
| y = 1.7732 | | | | | |
| 6.1836 | 0.8860 | 0.8860 | 0.8860 | 0.8860 | 0 |
| 6.8103 | .9130 | .8538 | .9130 | .8538 | .0296 |
| 7.4371 | .9541 | .8385 | .9541 | .8385 | .0578 |
| 8.0638 | .9699 | .7999 | .9699 | .7999 | .0850 |
| 8.6905 | .9757 | .7547 | .9757 | .7547 | .1105 |
| 9.9440 | .9730 | .6572 | .9730 | .6572 | .1579 |
| 11.1974 | .9504 | .5510 | .9504 | .5510 | .1997 |
| 12.4509 | .9118 | .4390 | .9118 | .4390 | .2364 |
| 13.7044 | .8608 | .3252 | .8608 | .3252 | .2678 |
| 16.2113 | .7296 | .1010 | .7296 | .1010 | .3143 |
| 18.7182 | .5665 | -.1127 | .5665 | -.1127 | .3396 |
| 21.2251 | .3794 | -.3062 | .3794 | -.3062 | .3428 |
| 23.7320 | .1616 | -.4638 | .1616 | -.4638 | .3127 |
| 26.2390 | -.0854 | -.5766 | -.0854 | -.5766 | .2456 |
| 28.7459 | -.3589 | -.6413 | -.3328 | -.6152 | .1412 |
| 31.2528 | -.6550 | -.6550 | -.565 | -.565 | 0 |
| y = 2.3642 | | | | | |
| 8.2449 | 0.6750 | 0.6750 | 0.6750 | 0.6750 | 0 |
| 8.8197 | .7066 | .6510 | .7066 | .6510 | .0278 |
| 9.3945 | .7490 | .6400 | .7490 | .6400 | .0545 |
| 9.9692 | .7759 | .6161 | .7759 | .6161 | .0799 |
| 10.5440 | .7843 | .5769 | .7843 | .5769 | .1037 |
| 11.6936 | .8001 | .5043 | .8001 | .5043 | .1479 |
| 12.8431 | .7917 | .4177 | .7917 | .4177 | .1870 |
| 13.9927 | .7730 | .3314 | .7730 | .3314 | .2208 |
| 15.1422 | .7416 | .2426 | .7416 | .2426 | .2495 |
| 17.4413 | .6475 | .0643 | .6475 | .0643 | .2916 |
| 19.7404 | .5215 | -.1045 | .5215 | -.1045 | .3130 |
| 22.0396 | .3675 | -.2581 | .3675 | -.2581 | .3128 |
| 24.3387 | .1819 | -.3827 | .1819 | -.3827 | .2823 |
| 26.6378 | -.0331 | -.4733 | -.0329 | -.4731 | .2201 |
| 28.9369 | -.2750 | -.5270 | -.2340 | -.4860 | .1260 |
| 31.2360 | -.5412 | -.5412 | -.428 | -.428 | 0 |

TABLE II.- WING COORDINATES - Continued

| $x_w$ | Unreflexed warped wing | | Reflexed warped wing | | Flat wing |
|---|---|---|---|---|---|
| | $z_u$ | $z_l$ | $z_u$ | $z_l$ | t/2 |
| y = 3.5463 | | | | | |
| 12.3674 | 0.3800 | 0.3800 | 0.3800 | 0.3800 | 0 |
| 12.8535 | .4181 | .3685 | .4181 | .3685 | .0248 |
| 13.3396 | .4592 | .3622 | .4592 | .3622 | .0485 |
| 13.8256 | .4950 | .3528 | .4950 | .3528 | .0711 |
| 14.3117 | .5135 | .3323 | .5135 | .3323 | .0906 |
| 15.2839 | .5435 | .2813 | .5435 | .2813 | .1311 |
| 16.2560 | .5543 | .2245 | .5543 | .2245 | .1649 |
| 17.2282 | .5563 | .1679 | .5563 | .1679 | .1942 |
| 18.2003 | .5448 | .1080 | .5448 | .1080 | .2184 |
| 20.1446 | .4960 | -.0084 | .4960 | -.0084 | .2522 |
| 22.0890 | .4150 | -.1186 | .4150 | -.1186 | .2668 |
| 24.0333 | .3051 | -.2159 | .3051 | -.2159 | .2605 |
| 25.9776 | .1665 | -.2953 | .1665 | -.2953 | .2309 |
| 27.9219 | .0015 | -.3535 | .0025 | -.3525 | .1775 |
| 29.8662 | -.1875 | -.3887 | -.1294 | -.3306 | .1006 |
| 31.8105 | -.3990 | -.3990 | -.250 | -.250 | 0 |
| y = 4.7284 | | | | | |
| 16.4897 | 0.1900 | 0.1900 | 0.1900 | 0.1900 | 0 |
| 16.9023 | .2326 | .1884 | .2326 | .1884 | .0221 |
| 17.3148 | .2722 | .1860 | .2722 | .1860 | .0431 |
| 17.7274 | .3069 | .1811 | .3069 | .1811 | .0629 |
| 18.1400 | .3351 | .1717 | .3351 | .1717 | .0817 |
| 18.9651 | .3672 | .1358 | .3672 | .1358 | .1157 |
| 19.7903 | .3925 | .1023 | .3925 | .1023 | .1451 |
| 20.6154 | .4012 | .0612 | .4012 | .0612 | .1700 |
| 21.4405 | .4040 | .0232 | .4040 | .0232 | .1904 |
| 23.0908 | .3811 | -.0541 | .3811 | -.0541 | .2176 |
| 24.7411 | .3286 | -.1252 | .3286 | -.1252 | .2269 |
| 26.3914 | .2494 | -.1864 | .2494 | -.1864 | .2179 |
| 28.0417 | .1461 | -.2355 | .1461 | -.2355 | .1908 |
| 29.6919 | .0202 | -.2706 | .0534 | -.2374 | .1454 |
| 31.3422 | -.1268 | -.2904 | -.0302 | -.1938 | .0818 |
| 32.9925 | -.2934 | -.2934 | -.100 | -.100 | 0 |

TABLE II.- WING COORDINATES - Continued

| $x_w$ | Unreflexed warped wing | | Reflexed warped wing | | Flat wing |
|---|---|---|---|---|---|
| | $z_u$ | $z_l$ | $z_u$ | $z_l$ | t/2 |
| y = 5.9105 | | | | | |
| 20.6122 | 0.0590 | 0.0590 | 0.0590 | 0.0590 | 0 |
| 20.9151 | .0982 | .0618 | .0982 | .0618 | .0182 |
| 21.2903 | .1345 | .0635 | .1345 | .0635 | .0355 |
| 21.6294 | .1648 | .0612 | .1648 | .0612 | .0518 |
| 21.9684 | .1931 | .0589 | .1931 | .0589 | .0671 |
| 22.6466 | .2394 | .0490 | .2394 | .0490 | .0952 |
| 23.3247 | .2645 | .0257 | .2645 | .0257 | .1194 |
| 24.0028 | .2830 | .0032 | .2830 | .0032 | .1399 |
| 24.6809 | .2895 | -.0239 | .2895 | -.0239 | .1567 |
| 26.0371 | .2872 | -.0708 | .2872 | -.0708 | .1790 |
| 27.3934 | .2593 | -.1137 | .2593 | -.1137 | .1865 |
| 28.7496 | .2083 | -.1497 | .211 | -.147 | .1790 |
| 30.1058 | .1363 | -.1771 | .1617 | -.1517 | .1567 |
| 31.4620 | .0447 | -.1941 | .1194 | -.1194 | .1194 |
| 32.8183 | -.0653 | -.1995 | .0871 | -.0471 | .0671 |
| 34.1745 | -.1929 | -.1929 | .040 | .040 | 0 |
| y = 7.0926 | | | | | |
| 24.7346 | 0 | 0 | 0 | 0 | 0 |
| 25.0002 | .0292 | .0008 | .0292 | .0008 | .0142 |
| 25.2657 | .0570 | .0014 | .0570 | .0014 | .0278 |
| 25.5312 | .0805 | -.0005 | .0805 | -.0005 | .0405 |
| 25.7968 | .1046 | -.0006 | .1046 | -.0006 | .0526 |
| 26.3279 | .1431 | -.0059 | .1431 | -.0059 | .0745 |
| 26.8590 | .1652 | -.0218 | .1652 | -.0218 | .0935 |
| 27.3901 | .1876 | -.0314 | .1876 | -.0314 | .1095 |
| 27.9212 | .2013 | -.0441 | .2013 | -.0441 | .1227 |
| 28.9834 | .2097 | -.0709 | .2097 | -.0709 | .1403 |
| 30.0456 | .1994 | -.0926 | .1994 | -.0926 | .1460 |
| 31.1079 | .1715 | -.1091 | .1753 | -.1053 | .1403 |
| 32.1701 | .1256 | -.1198 | .1527 | -.0927 | .1227 |
| 33.2323 | .0652 | -.1230 | .1341 | -.0541 | .0941 |
| 34.2945 | -.0119 | -.1171 | .1166 | -.0114 | .0526 |
| 35.3567 | -.1032 | -.1032 | .100 | .100 | 0 |

TABLE II.- WING COORDINATES - Continued

| $x_w$ | Unreflexed warped wing | | Reflexed warped wing | | Flat wing |
|---|---|---|---|---|---|
| | $z_u$ | $z_l$ | $z_u$ | $z_l$ | t/2 |
| y = 8.2747 | | | | | |
| 28.8570 | 0 | 0 | 0 | 0 | 0 |
| 29.0490 | .0243 | .0037 | .0243 | .0037 | .0103 |
| 29.2411 | .0461 | .0059 | .0461 | .0059 | .0201 |
| 29.4332 | .0663 | .0077 | .0663 | .0077 | .0293 |
| 29.6252 | .0840 | .0080 | .0840 | .0080 | .0380 |
| 30.0093 | .1119 | .0041 | .1119 | .0041 | .0539 |
| 30.3934 | .1384 | .0032 | .1384 | .0032 | .0676 |
| 30.7775 | .1535 | -.0049 | .1535 | -.0049 | .0792 |
| 31.1615 | .1660 | -.0114 | .1660 | -.0114 | .0887 |
| 31.9297 | .1876 | -.0152 | .1876 | -.0152 | .1014 |
| 32.6979 | .1881 | -.0231 | .1936 | -.0176 | .1056 |
| 33.4661 | .1780 | -.0248 | .1914 | -.0114 | .1014 |
| 34.2343 | .1559 | -.0215 | .1887 | .0113 | .0887 |
| 35.0024 | .1230 | -.0122 | .1826 | .0474 | .0676 |
| 35.7706 | .0798 | .0036 | .1720 | .0960 | .0380 |
| 36.5388 | .0262 | .0262 | .166 | .166 | 0 |
| y = 8.8658 | | | | | |
| 30.9182 | 0 | 0 | 0 | 0 | 0 |
| 31.0709 | .0172 | .0008 | .0172 | .0008 | .0082 |
| 31.2235 | .0335 | .0015 | .0335 | .0015 | .0160 |
| 31.3762 | .0488 | .0022 | .0488 | .0022 | .0233 |
| 31.5288 | .0632 | .0028 | .0632 | .0028 | .0302 |
| 31.8342 | .0923 | .0067 | .0923 | .0067 | .0428 |
| 32.1395 | .1147 | .0073 | .117 | .010 | .0537 |
| 32.4448 | .1320 | .0060 | .131 | .005 | .0630 |
| 32.7502 | .1445 | .0035 | .140 | 0 | .0705 |
| 33.3608 | .1601 | -.0011 | .162 | .002 | .0806 |
| 33.9714 | .1590 | -.0090 | .178 | .010 | .0840 |
| 34.5821 | .1531 | -.0081 | .186 | .026 | .0806 |
| 35.1928 | .1370 | -.0040 | .188 | .048 | .0705 |
| 35.8034 | .1117 | .0043 | .183 | .076 | .0537 |
| 36.4140 | .0792 | .0188 | .172 | .112 | .0302 |
| 37.0247 | .0390 | .0390 | .154 | .154 | 0 |

TABLE II.- WING COORDINATES - Continued

| $x_w$ | Unreflexed warped wing | | Reflexed warped wing | | Flat wing |
|---|---|---|---|---|---|
| | $z_u$ | $z_l$ | $z_u$ | $z_l$ | t/2 |
| y = 9.4569 | | | | | |
| 32.1887 | 0 | 0 | 0 | 0 | 0 |
| 32.3179 | .0095 | -.0045 | .0095 | -.0045 | .0070 |
| 32.4470 | .0185 | -.0085 | .0185 | -.0085 | .0135 |
| 32.5762 | .0197 | -.0122 | .0272 | -.0122 | .0197 |
| 32.7054 | .0351 | -.0151 | .0351 | -.0151 | .0256 |
| 32.9637 | .0482 | -.0252 | .0482 | -.0252 | .0362 |
| 33.2220 | .0597 | -.0313 | .0597 | -.0313 | .0455 |
| 33.4804 | .0693 | -.0373 | .0693 | -.0373 | .0533 |
| 33.7387 | .0772 | -.0422 | .0772 | -.0422 | .0597 |
| 34.2554 | .0894 | -.0470 | .0894 | -.0470 | .0682 |
| 34.7720 | .0928 | -.0492 | .0960 | -.0460 | .0710 |
| 35.2887 | .0894 | -.0470 | .0982 | -.0382 | .0682 |
| 35.8054 | .0737 | -.0329 | .1013 | -.0053 | .0533 |
| 36.3221 | .0627 | -.0283 | .1055 | .0145 | .0455 |
| 36.8387 | .0390 | -.0122 | .1036 | .0524 | .0256 |
| 37.3554 | .0090 | .0090 | .095 | .095 | 0 |
| y = 10.6390 | | | | | |
| 34.7207 | 0 | 0 | 0 | 0 | 0 |
| 34.8029 | .004 | -.004 | -.0023 | -.0111 | .0044 |
| 34.8850 | .010 | -.008 | -.0032 | -.0204 | .0086 |
| 34.9672 | .015 | -.011 | -.0029 | -.0281 | .0126 |
| 35.0494 | .019 | -.014 | -.0024 | -.0348 | .0162 |
| 35.2137 | .027 | -.019 | .0031 | -.0429 | .0230 |
| 35.3781 | .034 | -.024 | .0105 | -.0475 | .0290 |
| 35.5424 | .038 | -.030 | .0189 | -.0489 | .0339 |
| 35.7068 | .038 | -.038 | .0274 | -.0486 | .0380 |
| 36.0355 | .040 | -.048 | .0378 | -.0490 | .0434 |
| 36.3642 | .037 | -.053 | .0351 | -.0553 | .0452 |
| 36.6929 | .031 | -.055 | .0314 | -.0554 | .0434 |
| 37.0216 | .021 | -.055 | .0280 | -.0480 | .0380 |
| 37.3503 | .009 | -.049 | .0210 | -.0370 | .0290 |
| 37.6790 | -.007 | -.039 | .0162 | -.0162 | .0162 |
| 38.0077 | -.026 | -.026 | .010 | .010 | 0 |

TABLE II.- WING COORDINATES - Concluded

| $x_w$ | Unreflexed warped wing | | Reflexed warped wing | | Flat wing |
|---|---|---|---|---|---|
| | $z_u$ | $z_l$ | $z_u$ | $z_l$ | t/2 |
| y = 11.2300 | | | | | |
| 35.9882 | 0 | 0 | 0 | 0 | 0 |
| 36.0469 | .005 | -.001 | -.0017 | -.0079 | .0031 |
| 36.1056 | .009 | -.003 | -.0028 | -.0150 | .0061 |
| 36.1642 | .013 | -.005 | -.0035 | -.0215 | .0090 |
| 36.2229 | .017 | -.007 | -.0039 | -.0273 | .0117 |
| 36.3403 | .020 | -.012 | -.0038 | -.0368 | .0165 |
| 36.4576 | .024 | -.018 | -.0026 | -.0438 | .0206 |
| 36.5750 | .026 | -.022 | -.0006 | -.0490 | .0242 |
| 36.6924 | .027 | -.027 | .0019 | -.0523 | .0271 |
| 36.9271 | .026 | -.036 | .0075 | -.0545 | .0310 |
| 37.1618 | .022 | -.042 | .0119 | -.0527 | .0323 |
| 37.3965 | .016 | -.046 | .0122 | -.0498 | .0310 |
| 37.6312 | .007 | -.047 | .0071 | -.0471 | .0271 |
| 37.8660 | -.004 | -.046 | .0036 | -.0376 | .0206 |
| 38.1007 | -.018 | -.092 | -.0033 | -.0267 | .0117 |
| 38.3354 | -.032 | -.032 | -.010 | -.010 | 0 |
| y = 11.8211 | | | | | |
| 37.2557 | 0 | 0 | 0 | 0 | 0 |
| 37.2909 | .003 | -.001 | .003 | -.001 | .0019 |
| 37.3261 | .006 | -.002 | .006 | -.002 | .0037 |
| 37.3612 | .008 | -.002 | .008 | -.002 | .0054 |
| 37.3964 | .010 | -.004 | .010 | -.004 | .0070 |
| 37.4668 | .013 | -.007 | .013 | -.007 | .0099 |
| 37.5371 | .014 | -.010 | .014 | -.010 | .0124 |
| 37.6075 | .016 | -.012 | .016 | -.012 | .0145 |
| 37.6778 | .017 | -.015 | .017 | -.015 | .0162 |
| 37.8185 | .019 | -.018 | .019 | -.018 | .0186 |
| 37.9592 | .019 | -.019 | .019 | -.019 | .0193 |
| 38.1000 | .017 | -.021 | .017 | -.021 | .0186 |
| 38.2407 | .012 | -.020 | .012 | -.020 | .0162 |
| 38.3814 | .006 | -.018 | .006 | -.018 | .0124 |
| 38.5221 | -.001 | -.015 | -.001 | -.015 | .0070 |
| 38.6628 | -.010 | -.010 | -.010 | -.010 | 0 |

TABLE III.- BODY COORDINATES

| Longitudinal station, x, in. | Flat and cambered body radii, r, in. | Cambered body vertical offset, $z_B$, in. |
|---|---|---|
| 0 | 0 | 2.520 |
| .866 | .168 | 2.520 |
| 1.732 | .286 | 2.520 |
| 2.597 | .378 | 2.520 |
| 3.463 | .464 | 2.520 |
| 4.329 | .539 | 2.520 |
| 5.195 | .611 | 2.520 |
| 6.061 | .670 | 2.520 |
| 6.926 | .725 | 2.520 |
| 7.792 | .775 | 2.520 |
| 8.658 | .823 | 2.520 |
| 9.524 | .865 | 2.520 |
| 10.390 | .904 | 2.520 |
| 11.255 | .939 | 2.520 |
| 12.121 | .970 | 2.490 |
| 12.255 | .975 | 2.486 |
| 12.987 | .992 | 2.435 |
| 13.255 | .995 | 2.415 |
| 13.853 | 1.002 | 2.360 |
| 14.286 | 1.010 | 2.310 |
| 15.255 | 1.010 | 2.205 |
| 17.255 | 1.010 | 1.970 |
| 19.255 | 1.010 | 1.732 |
| 21.255 | 1.010 | 1.494 |
| 23.255 | 1.010 | 1.257 |
| 25.255 | 1.010 | 1.018 |
| 27.255 | 1.010 | .779 |
| 29.255 | 1.010 | .540 |
| 31.255 | 1.010 | .320 |
| 33.255 | 1.000 | .110 |
| 35.255 | .970 | -.070 |
| 37.255 | .920 | -.240 |
| 39.255 | .860 | -.400 |
| 40.255 | .835 | -.475 |
| 41.255 | .805 | -.535 |
| 42.255 | .770 | -.600 |
| 43.255 | .750 | -.660 |

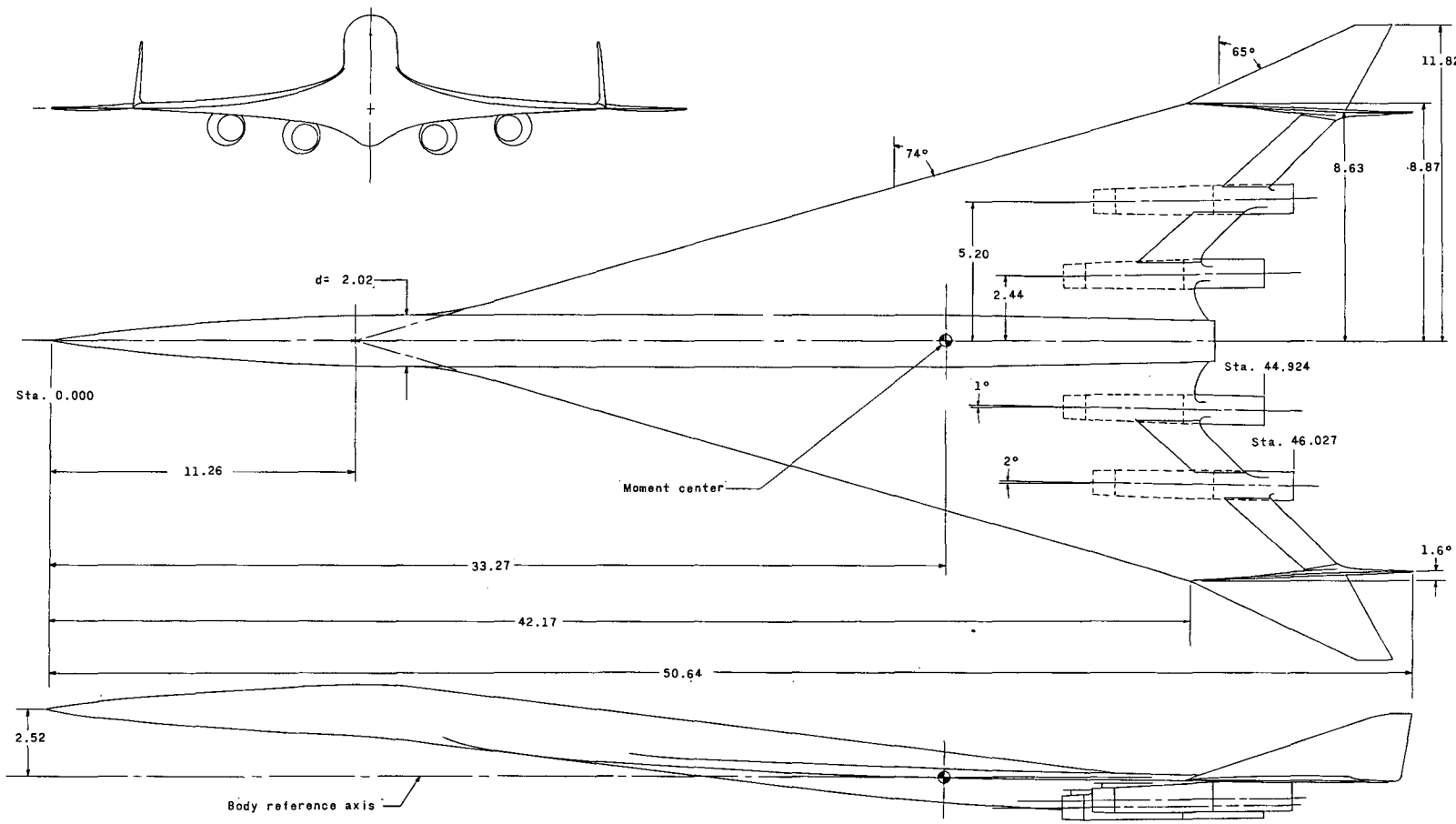


(a) Complete configuration.

Figure 1.- Details of model. All linear dimensions are in inches.

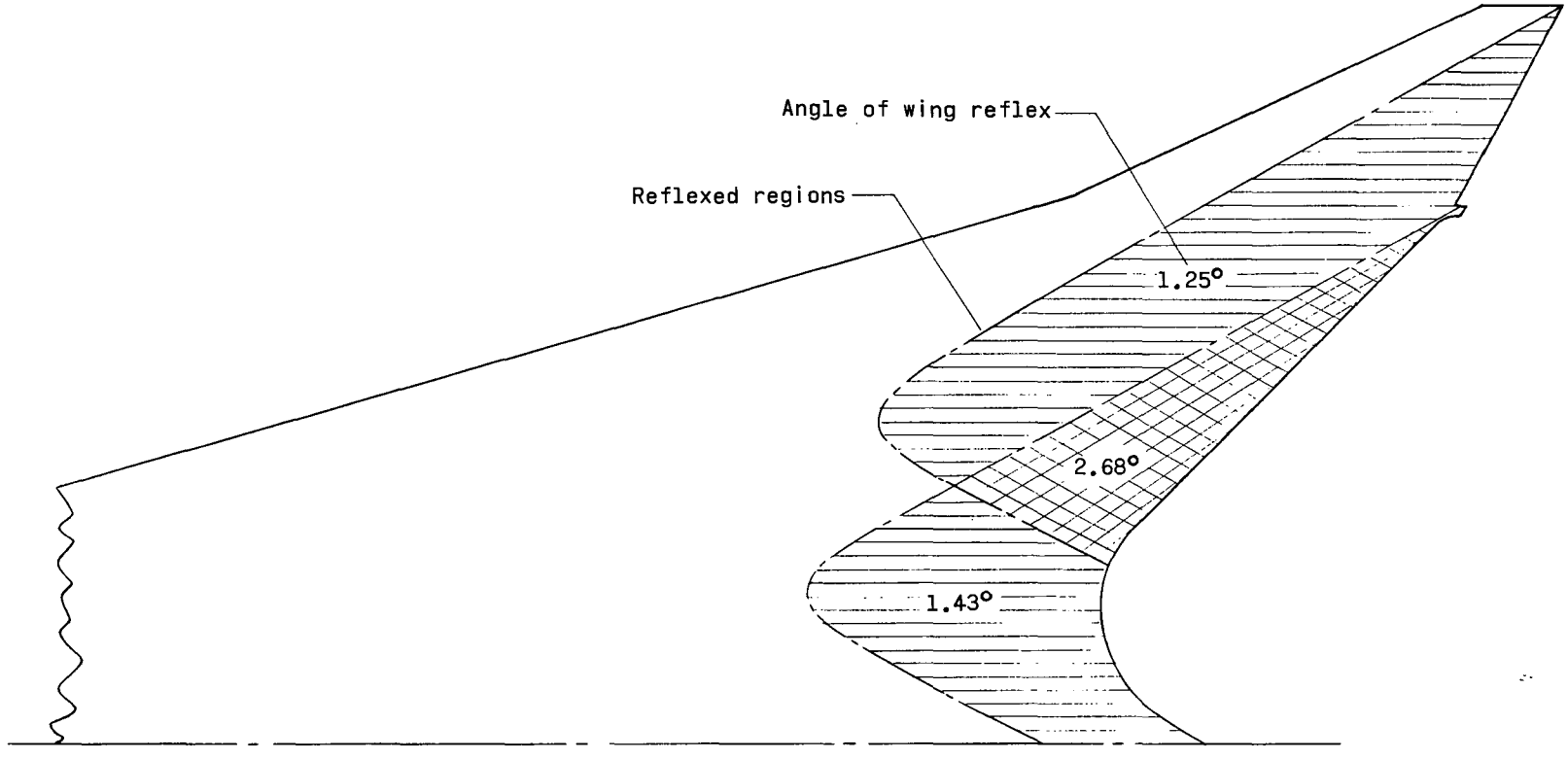


(b) Reflexed section of wing trailing edge.

Figure 1.- Continued.

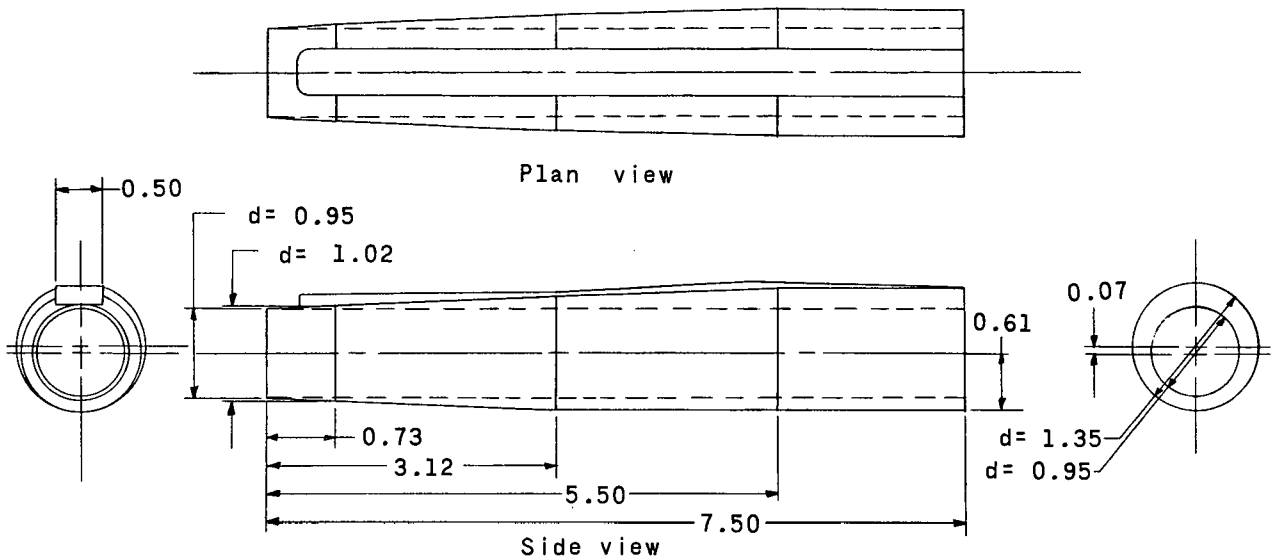


(c) Details of inboard and outboard nacelles.

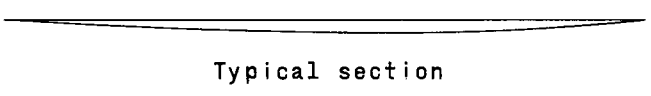


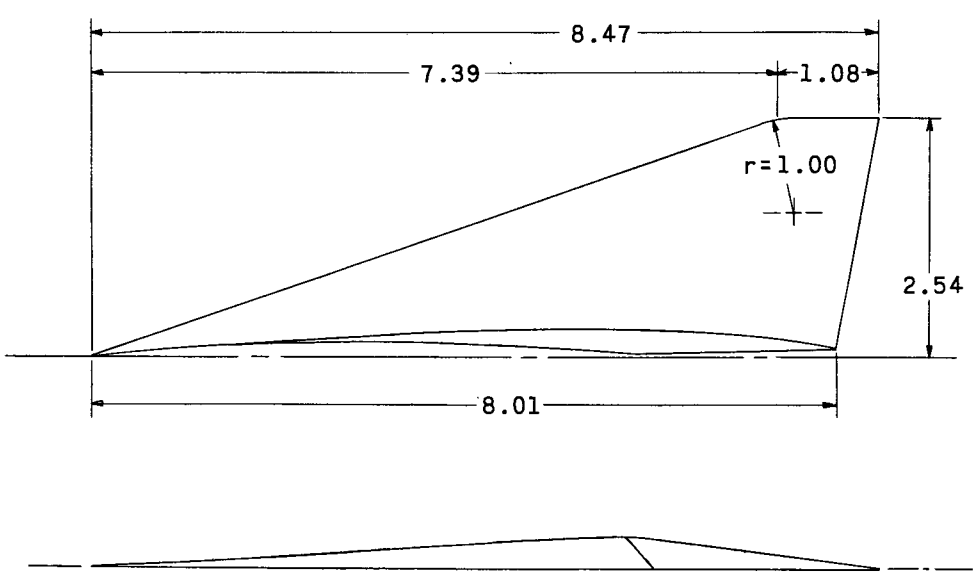


(d) Details of vertical tail.

Figure 1.- Continued.

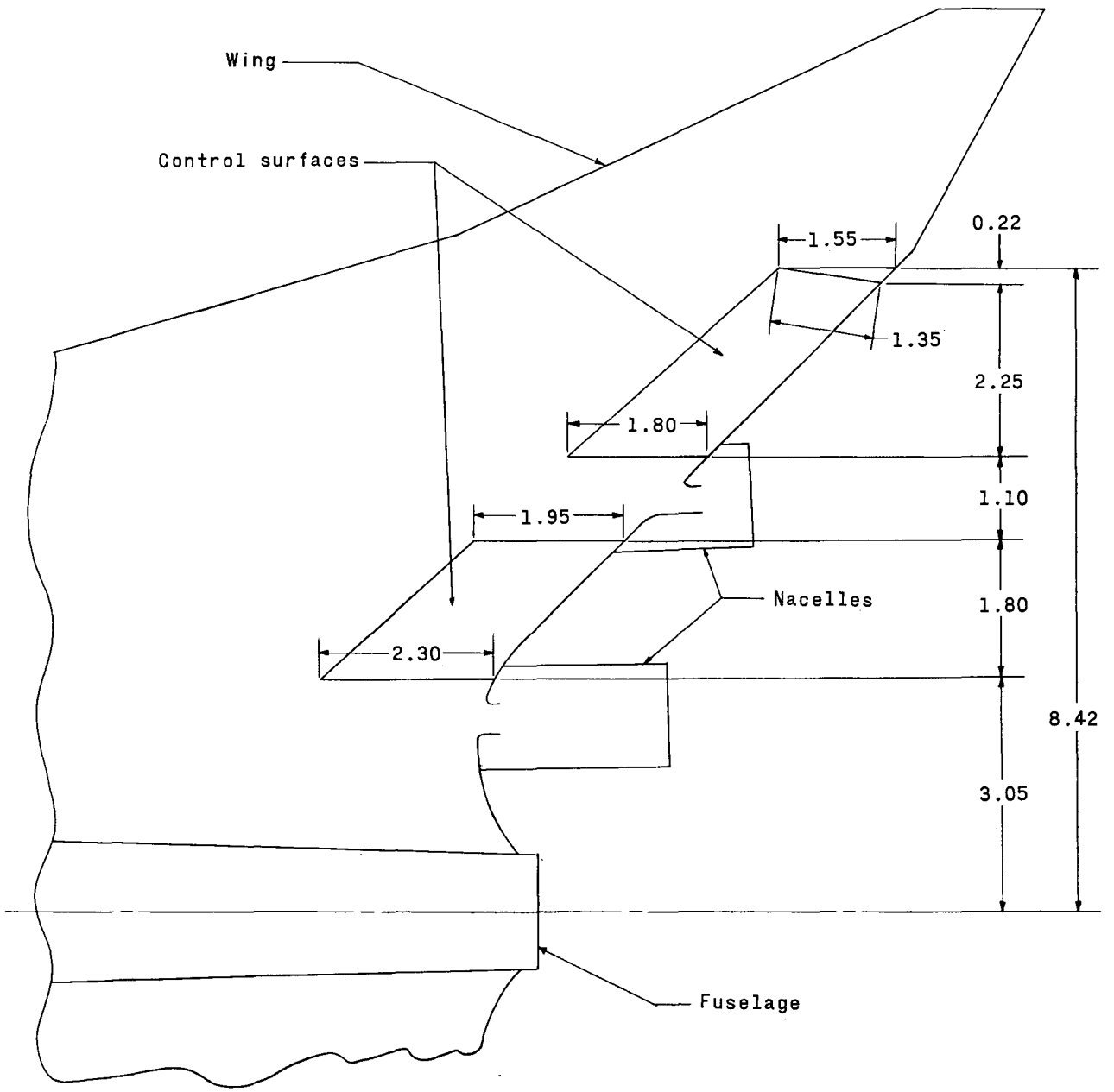


(e) Details of wing trailing-edge controls.

Figure 1.- Continued.

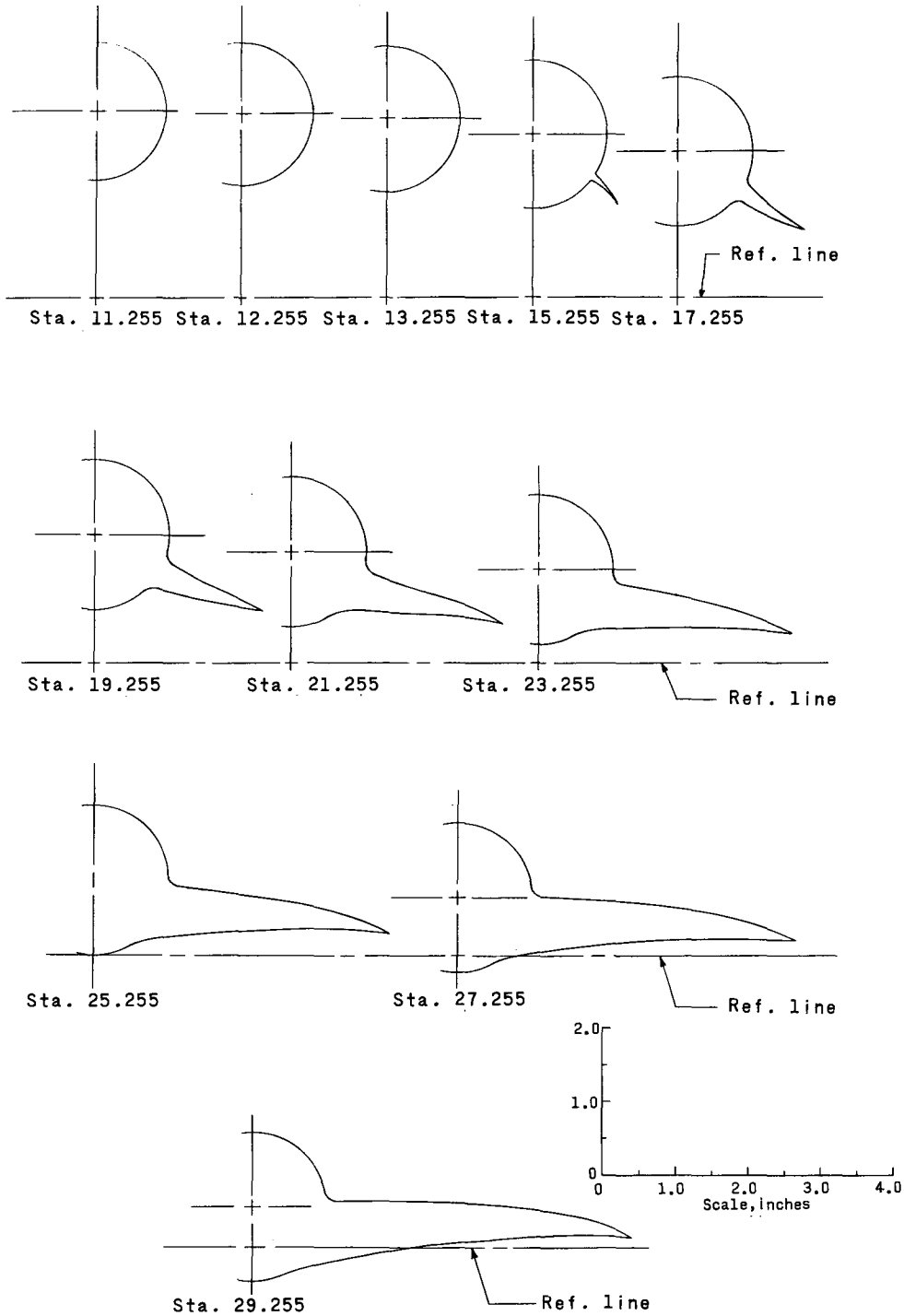


(f) Cross sections of forward longitudinal stations.

Figure 1.- Continued.

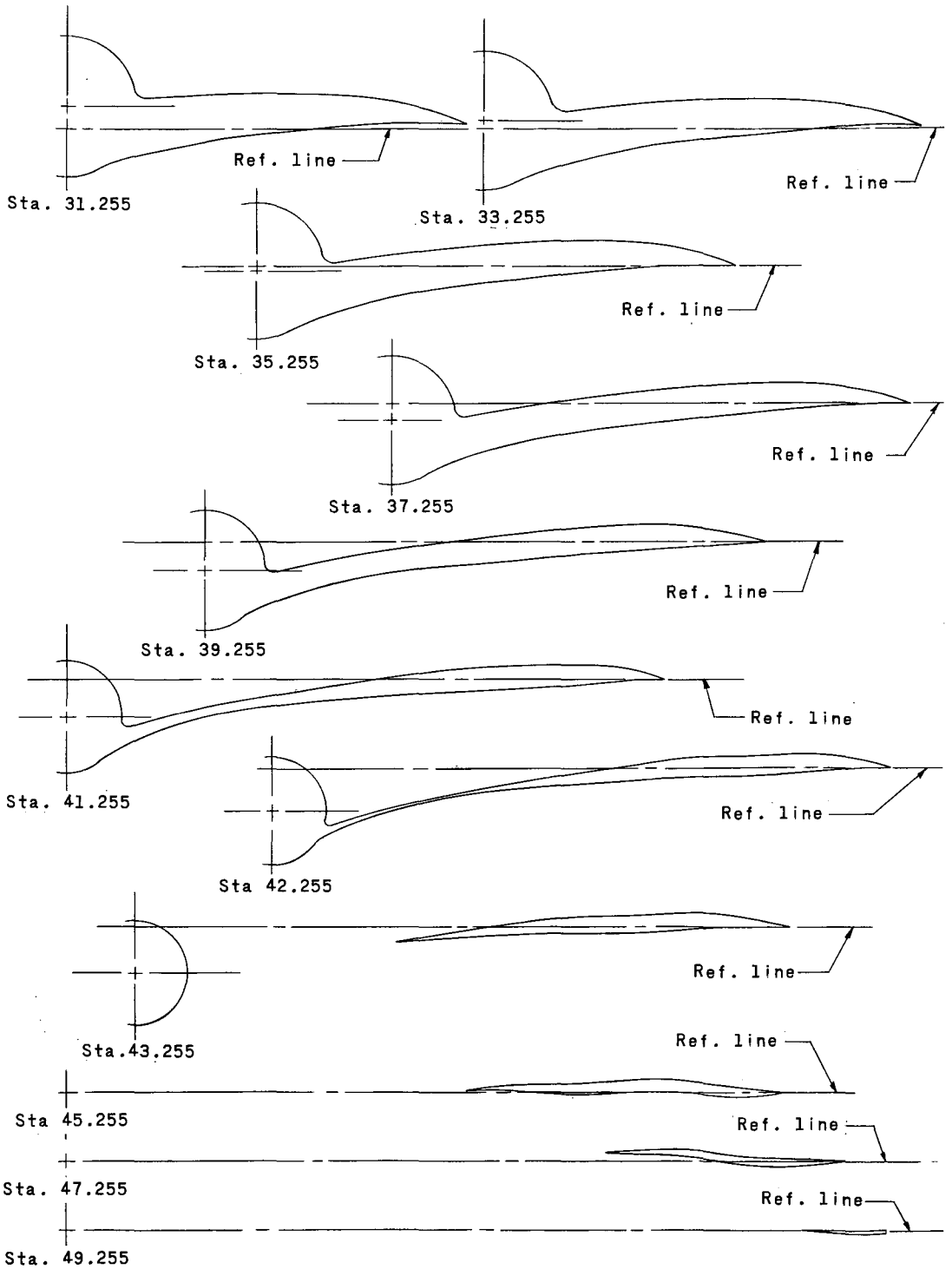


(g) Cross sections of rearward longitudinal stations.

Figure 1.- Concluded.

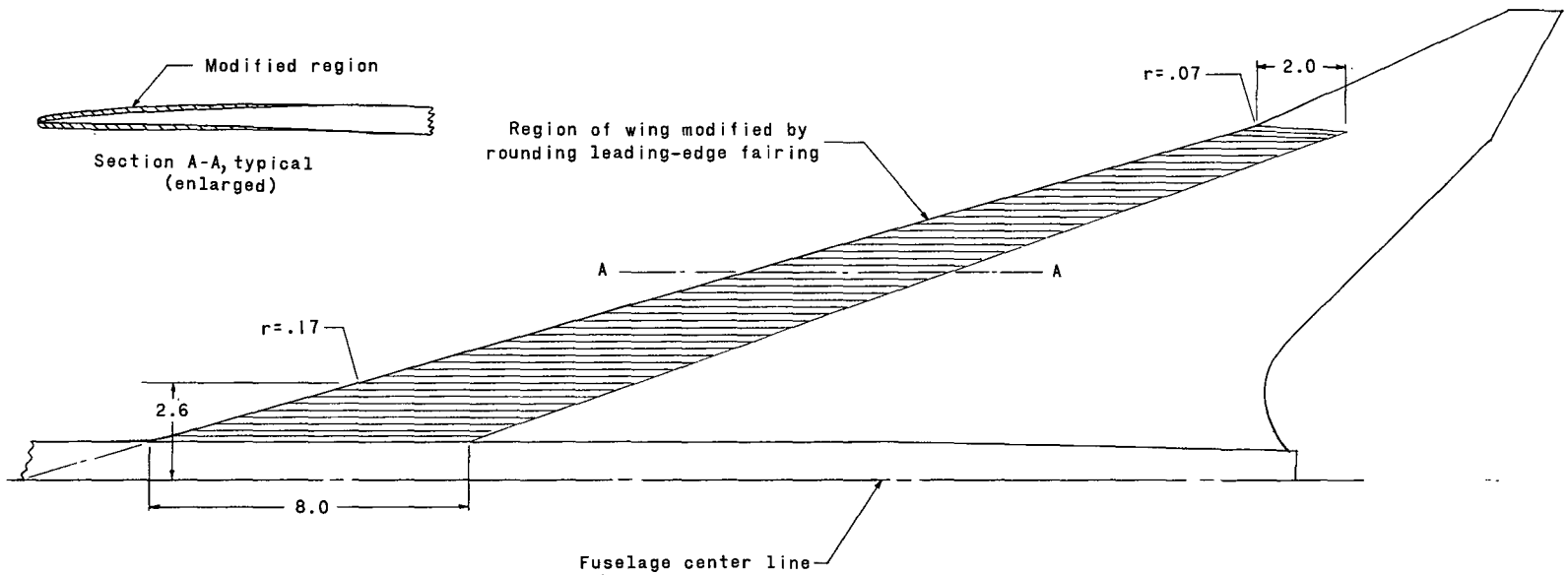


Figure 2.- Details of wing rounded-leading-edge modification on warped-wing—body combination.

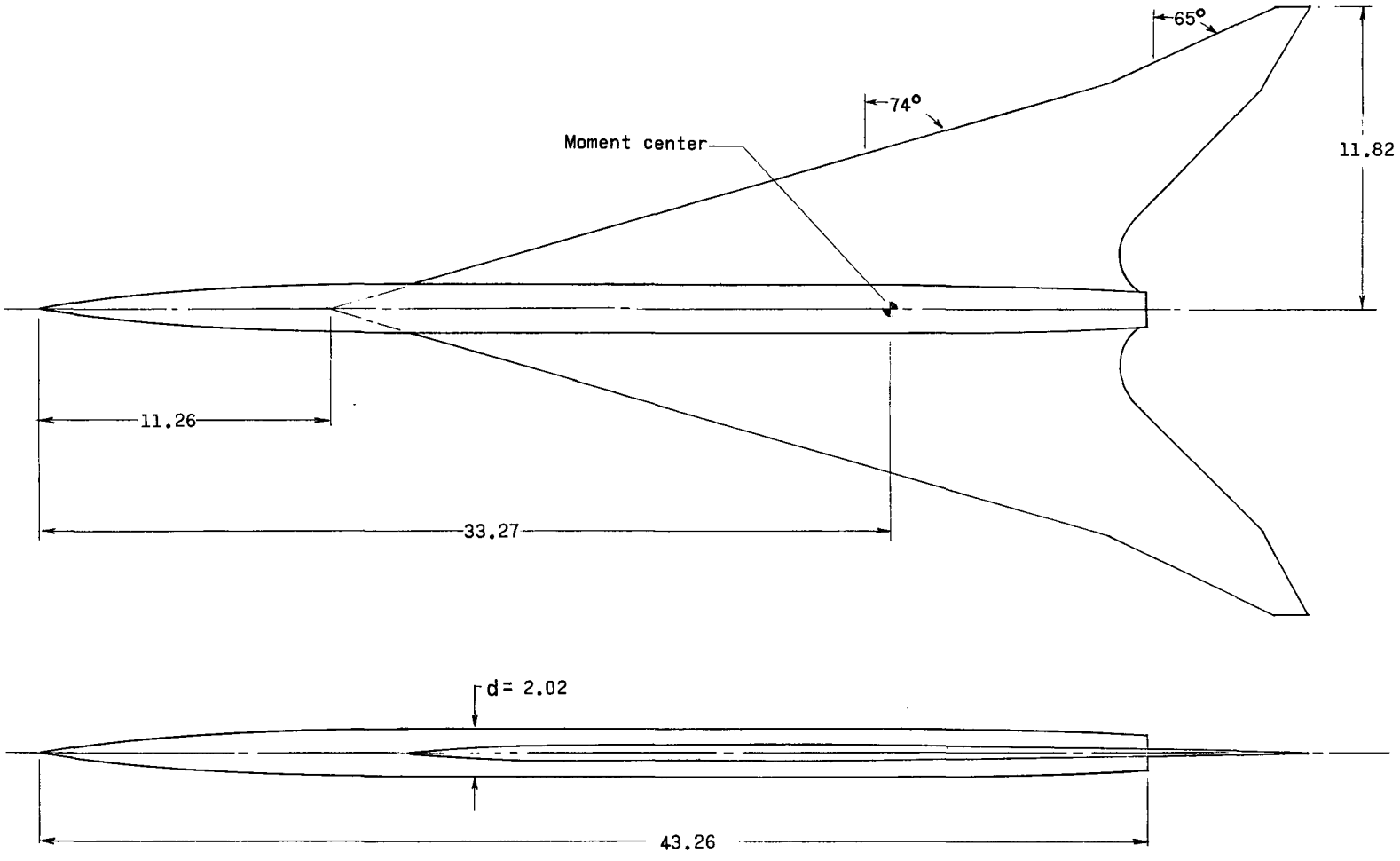


Figure 3.- Flat-wing—body model.

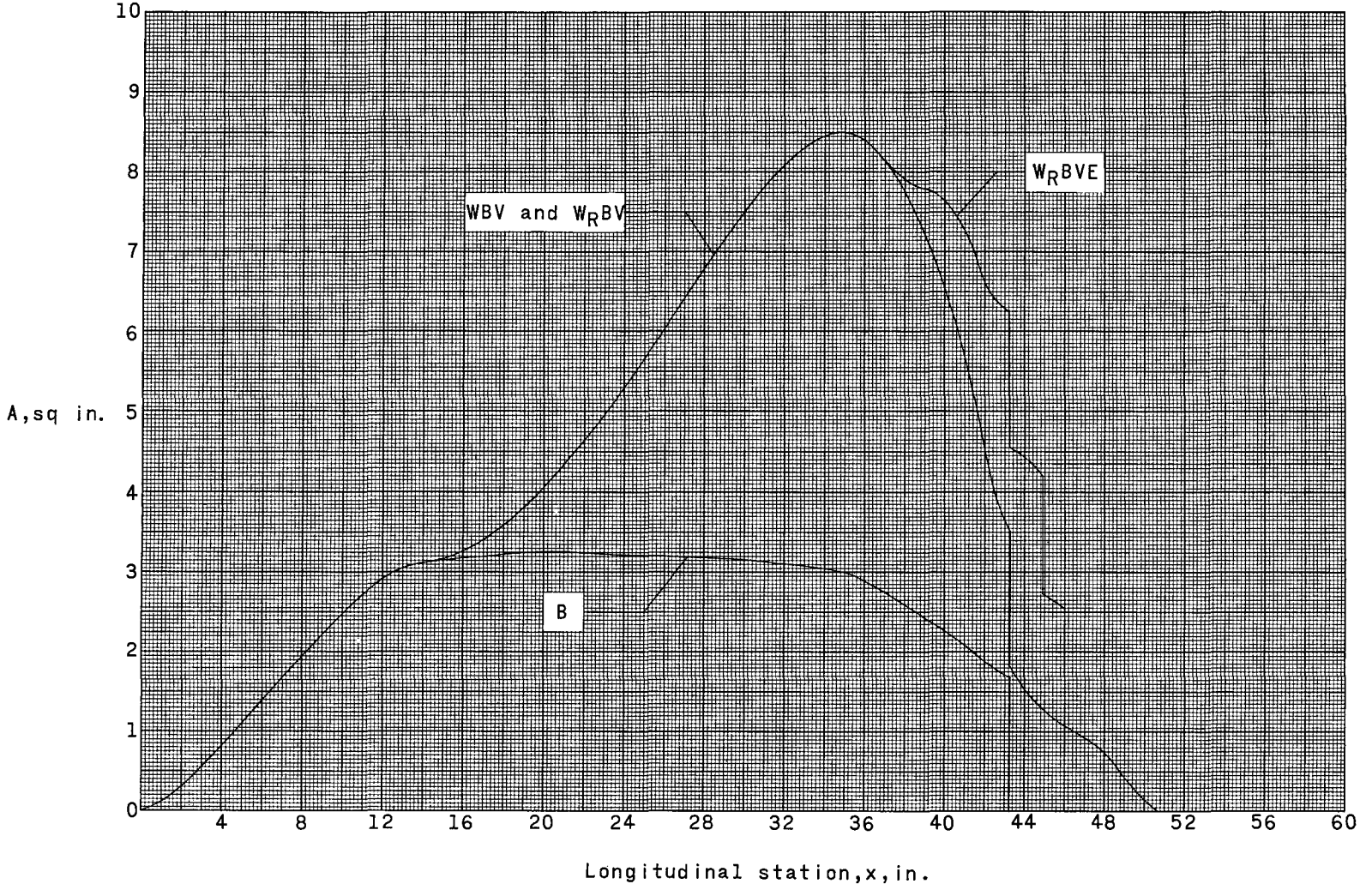


Figure 4.- Normal cross-sectional area for the various model components.

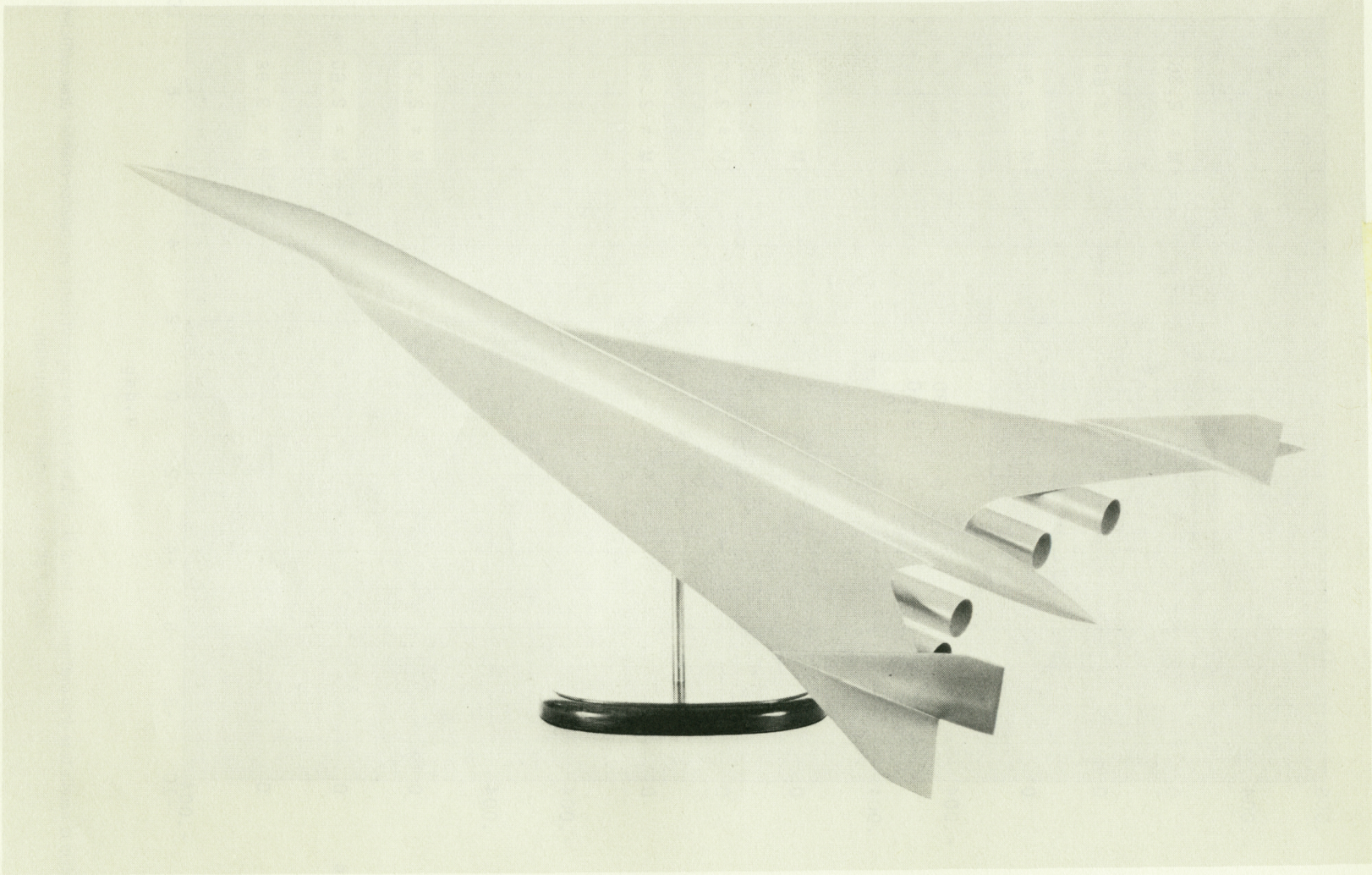

Figure 5.- Photograph of a model of complete aircraft configuration.

L-64-4963

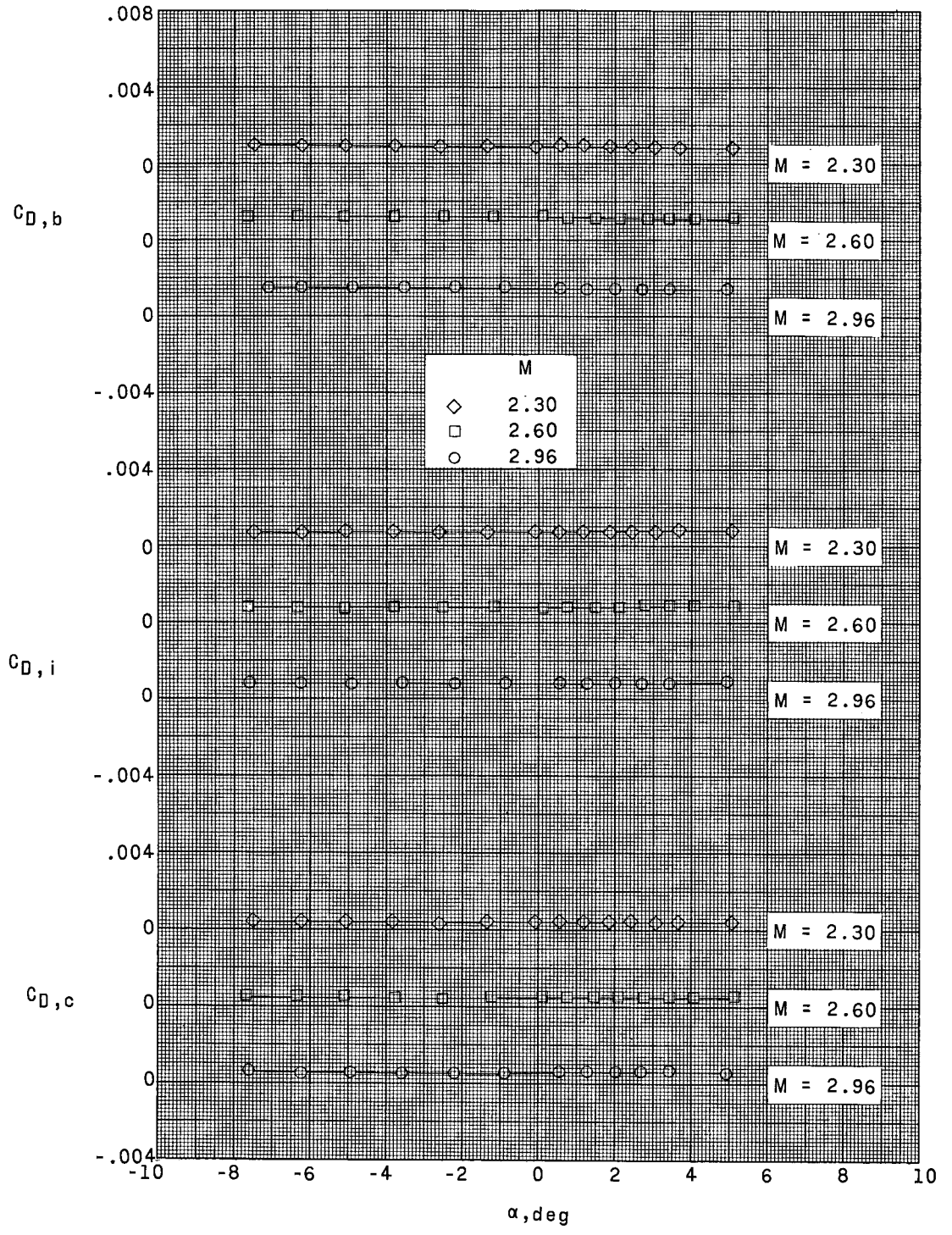


Figure 6.- Variation of nacelle base drag coefficient, internal skin-friction nacelle drag coefficient, and balance-chamber drag coefficient with angle of attack for complete configuration.

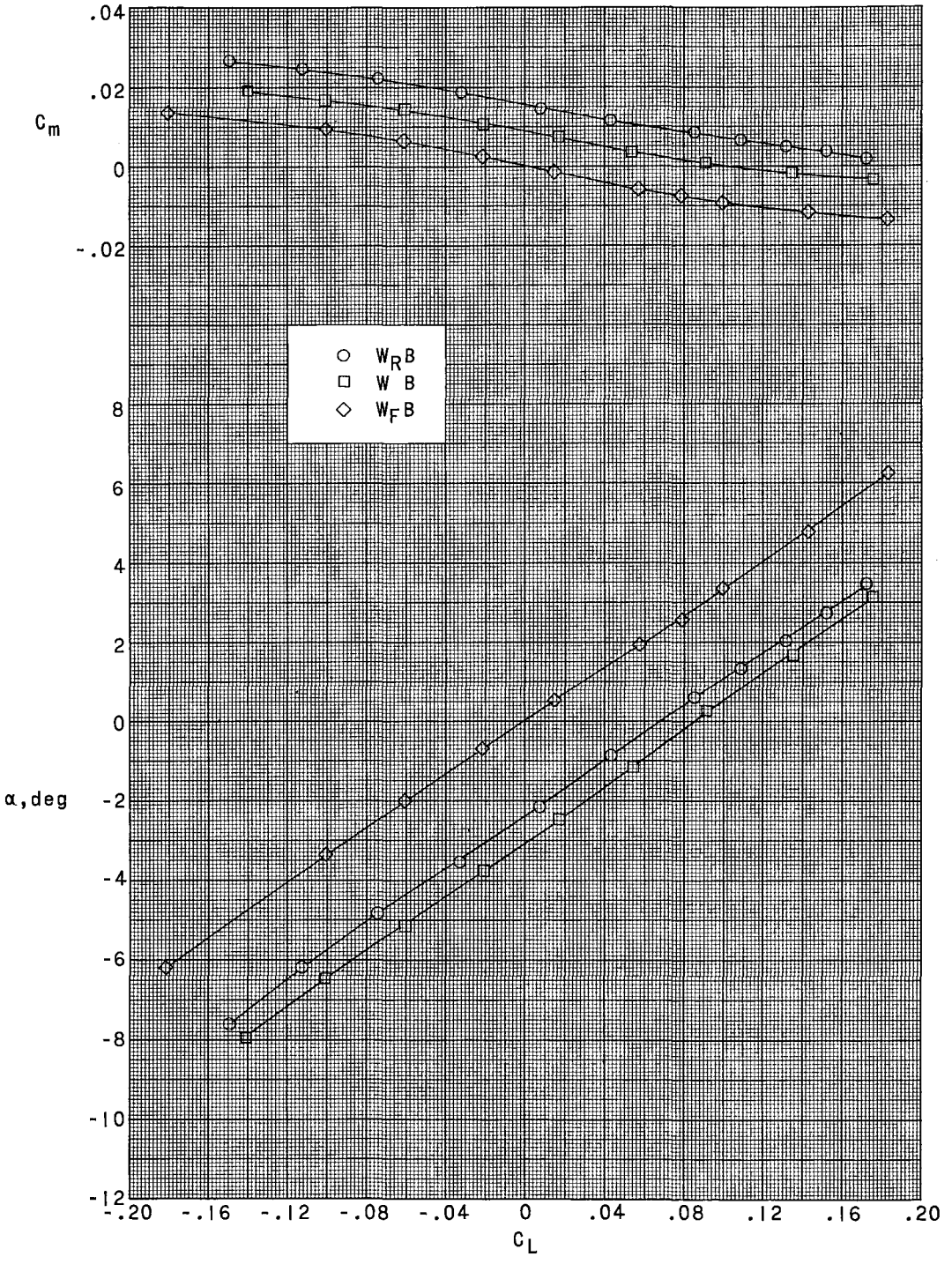


(a) M = 2.30.

Figure 7.- Comparison of longitudinal aerodynamic characteristics for three wing-body models.

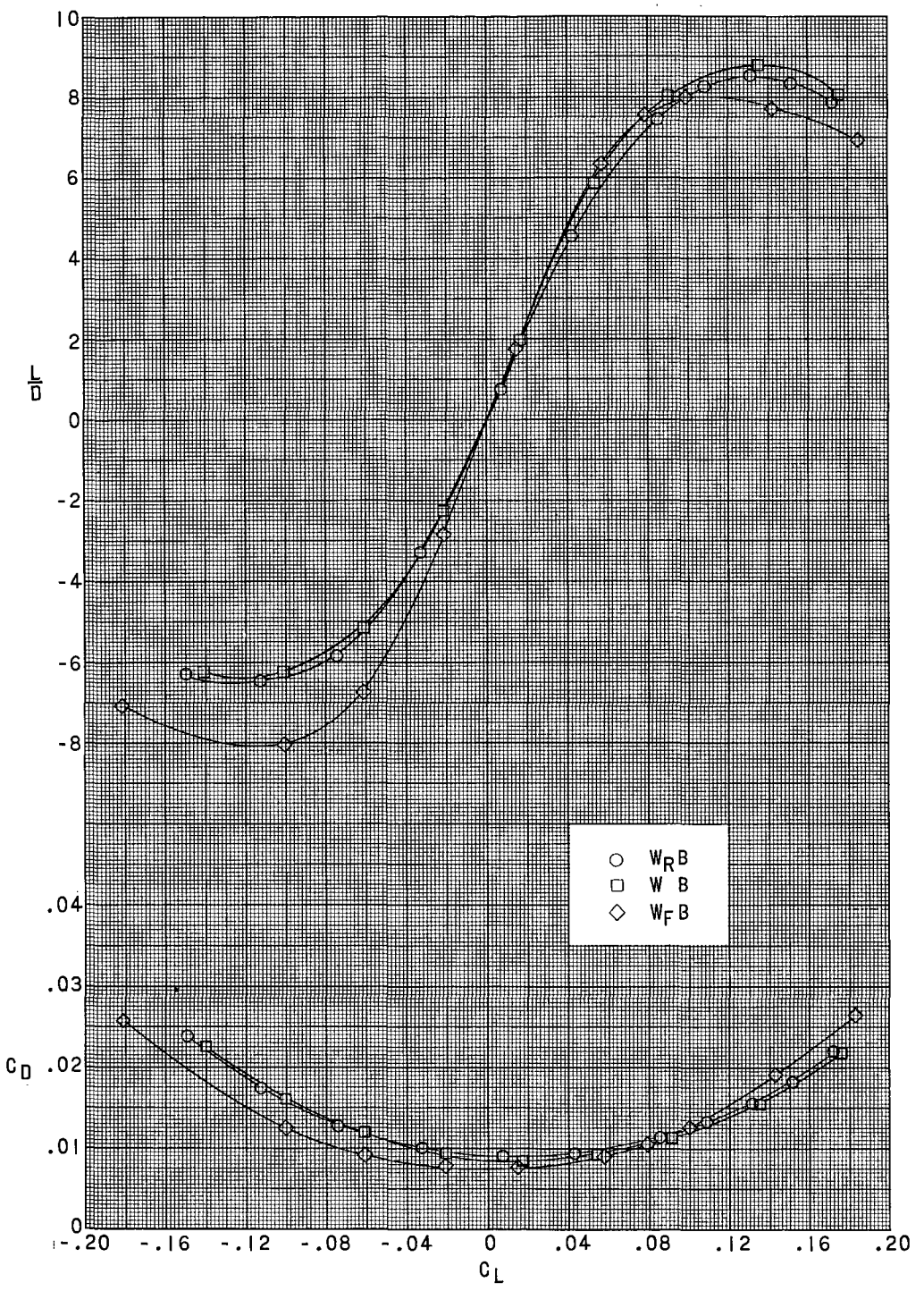


(a) Concluded.

Figure 7.- Continued.

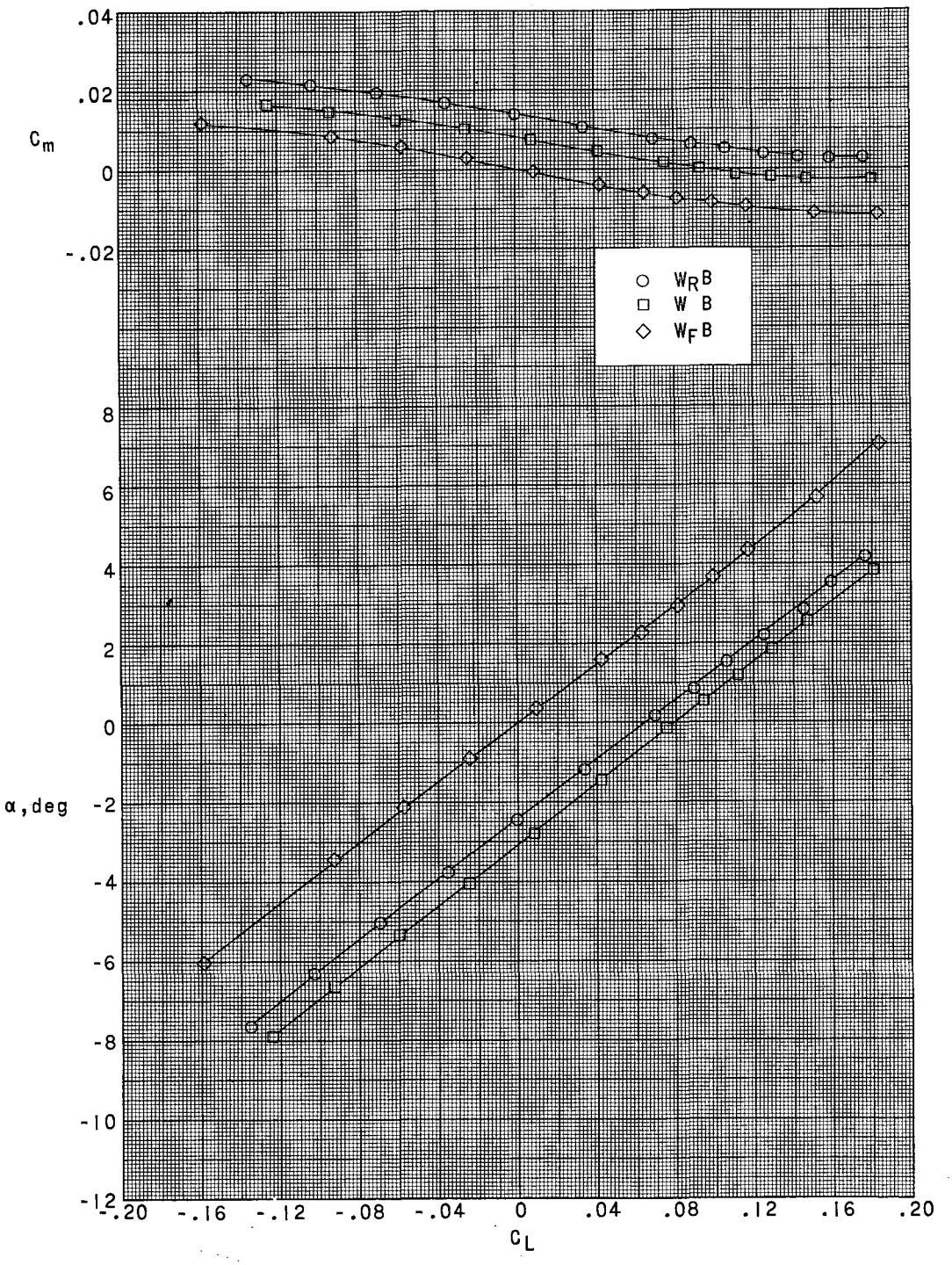


(b) M = 2.60.

Figure 7.- Continued.

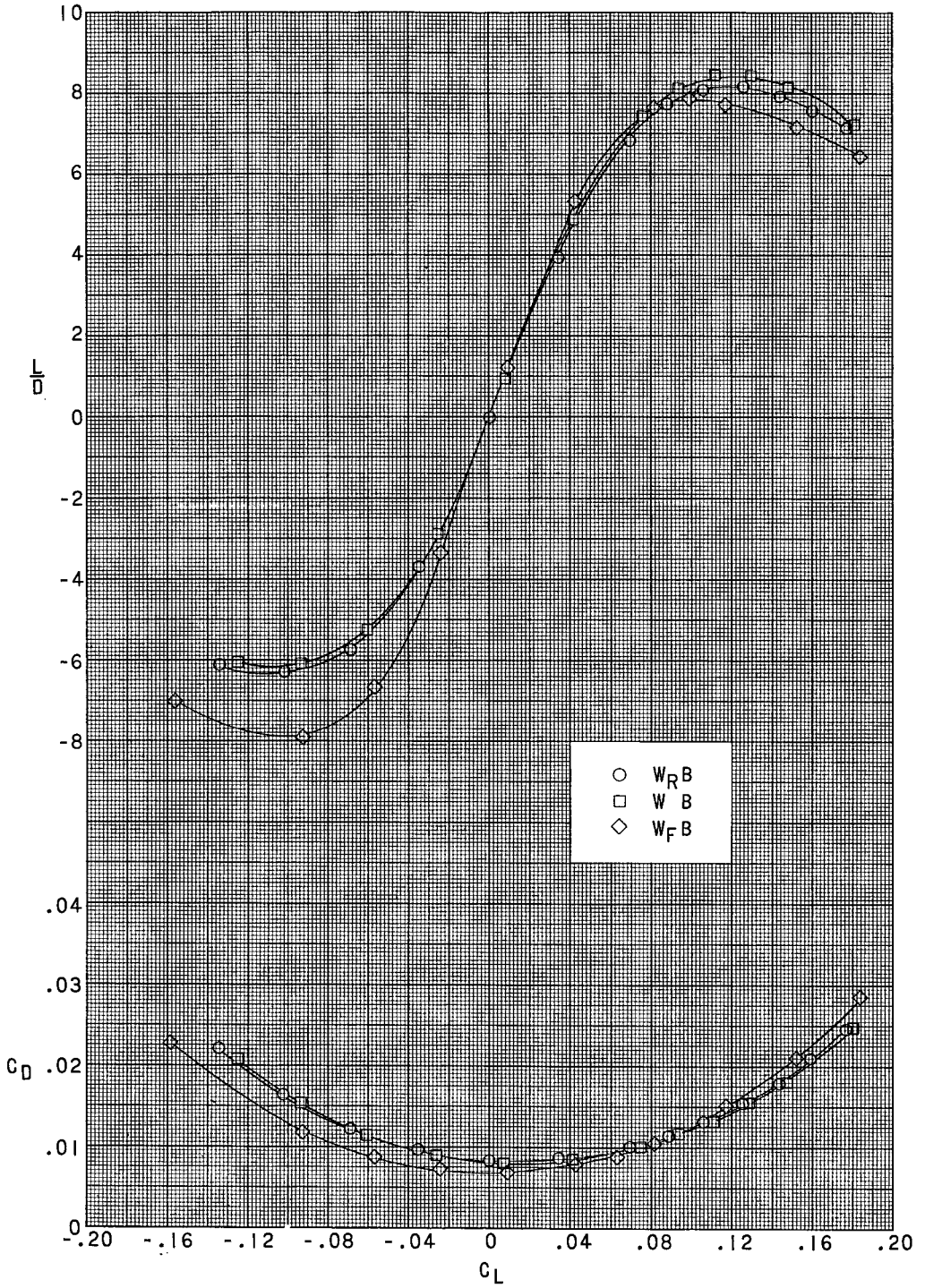


(b) Concluded.

Figure 7.- Continued.

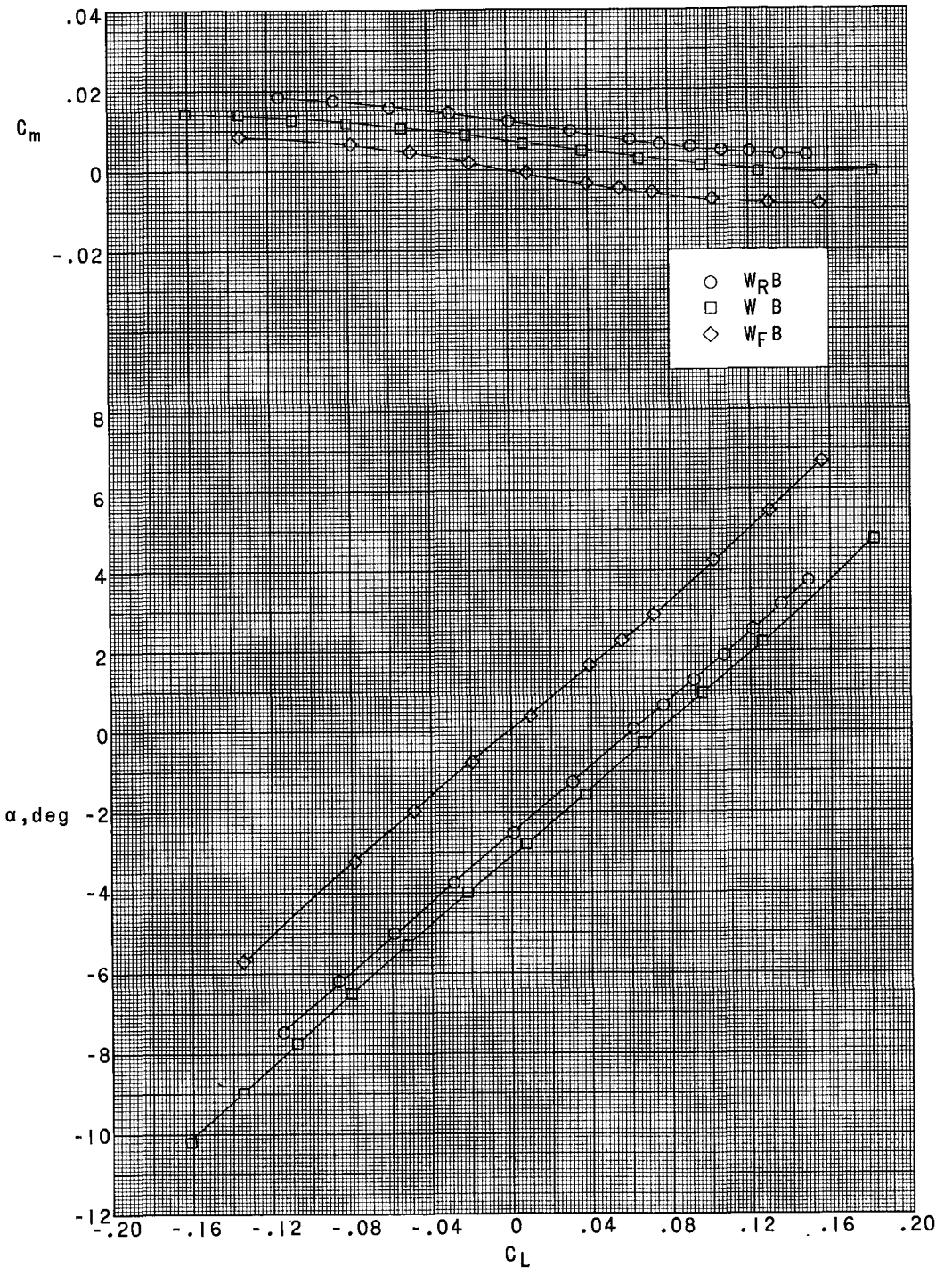


(c) M = 2.96.

Figure 7.- Continued.

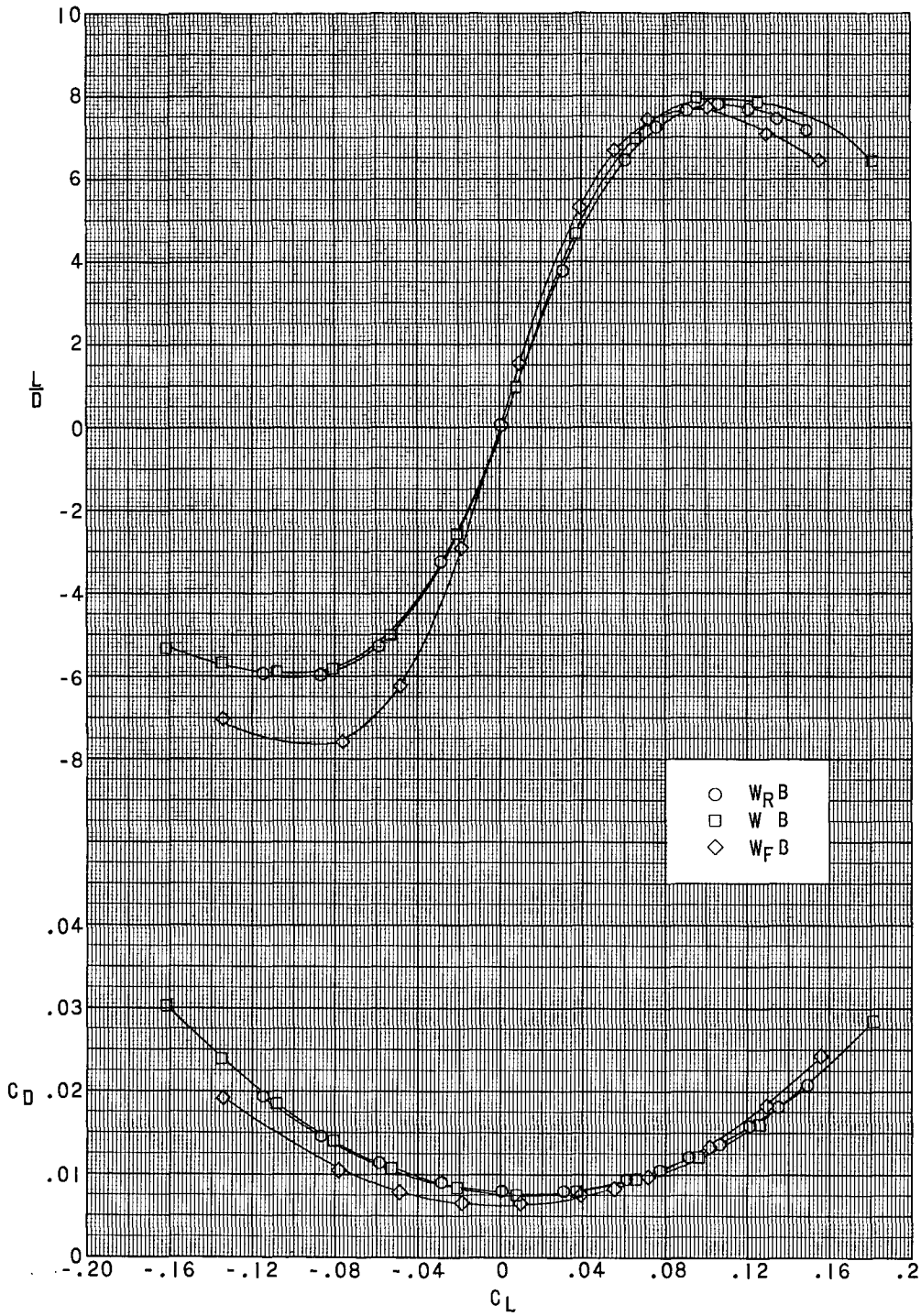


(c) Concluded.

Figure 7.- Concluded.

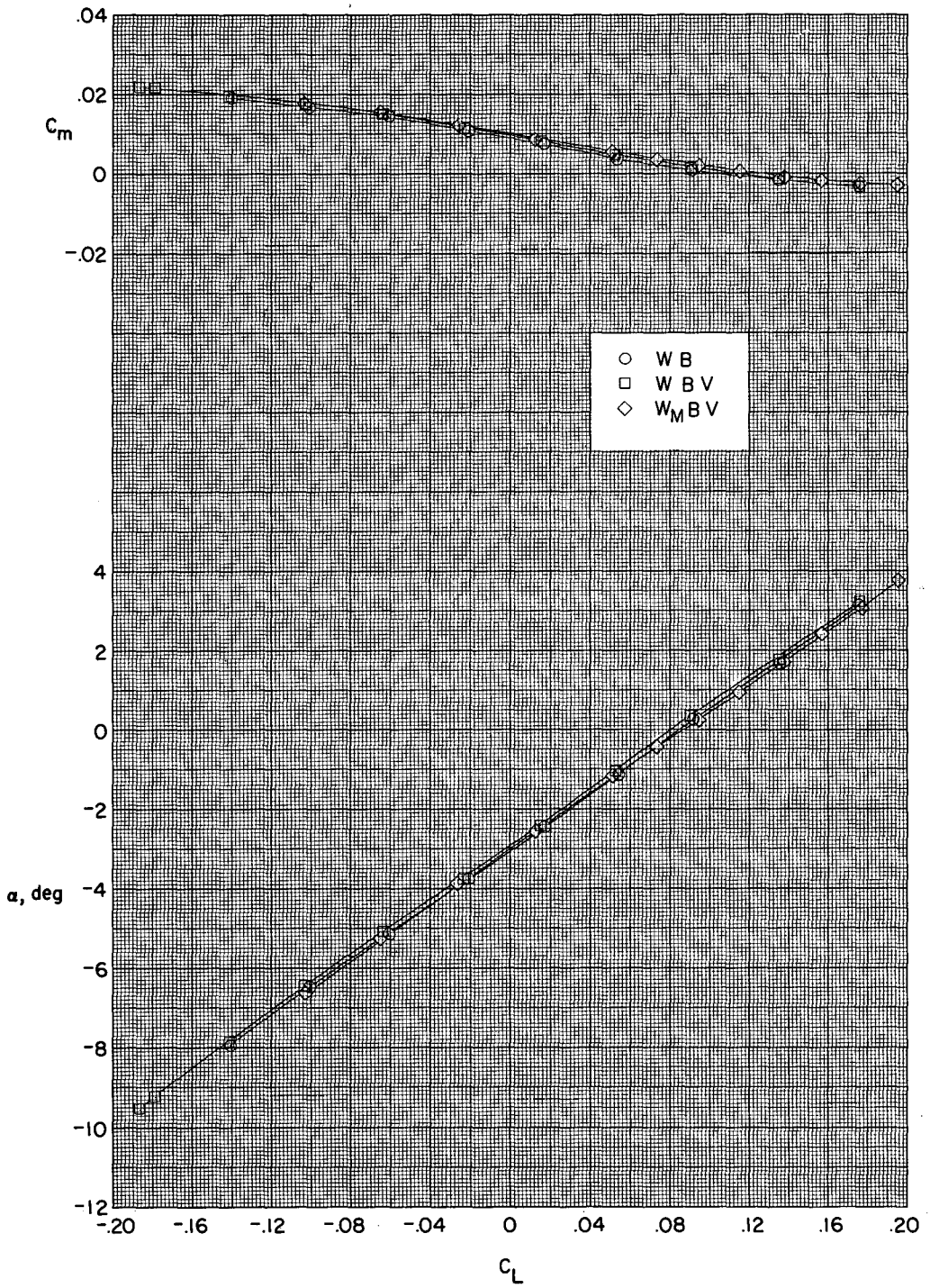


(a) M = 2.30.

Figure 8.- Effect of vertical tails and modified rounded wing leading edge on longitudinal aerodynamic characteristics for unreflexed-warped-wing model.

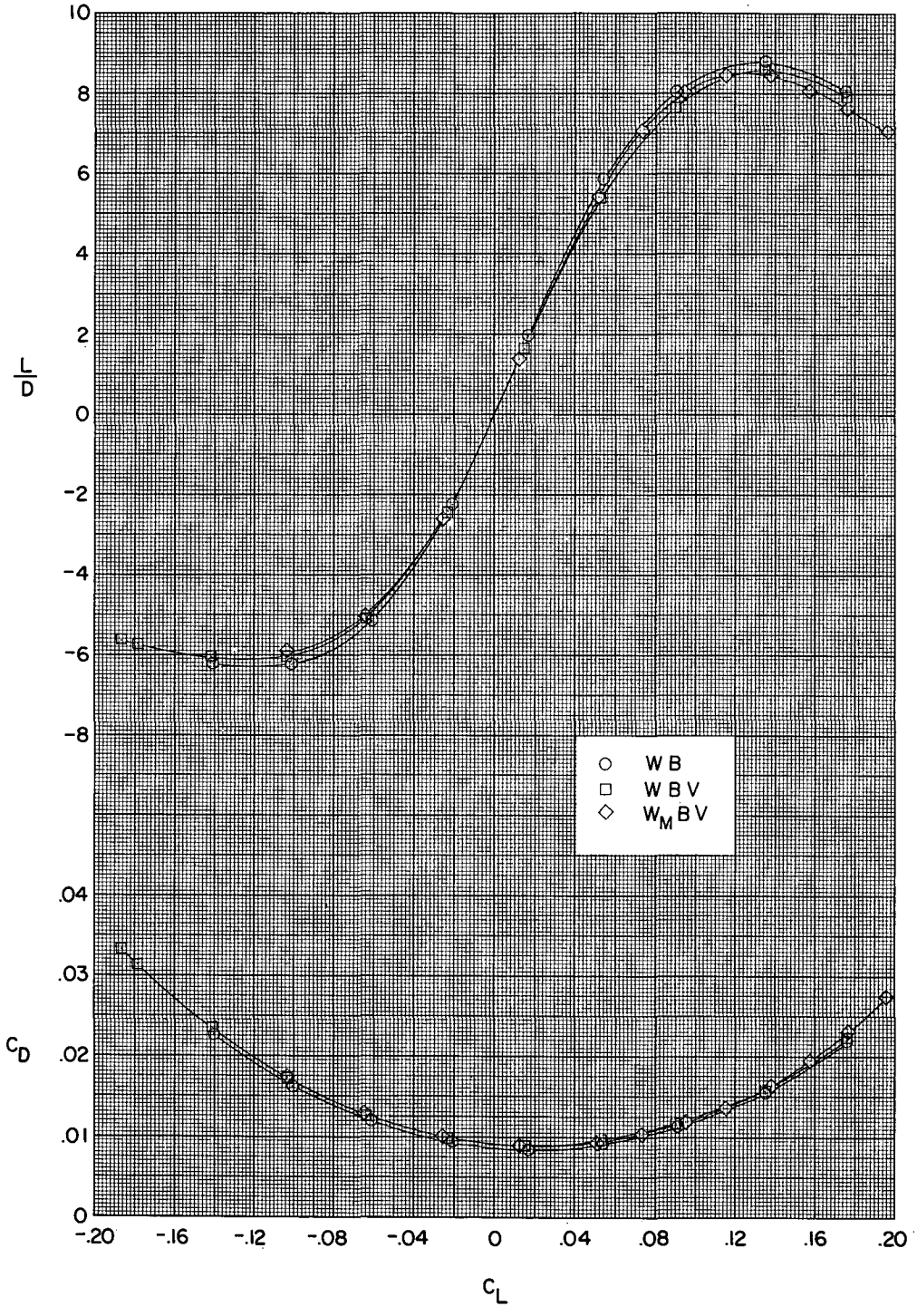


(a) Concluded.

Figure 8.- Continued.

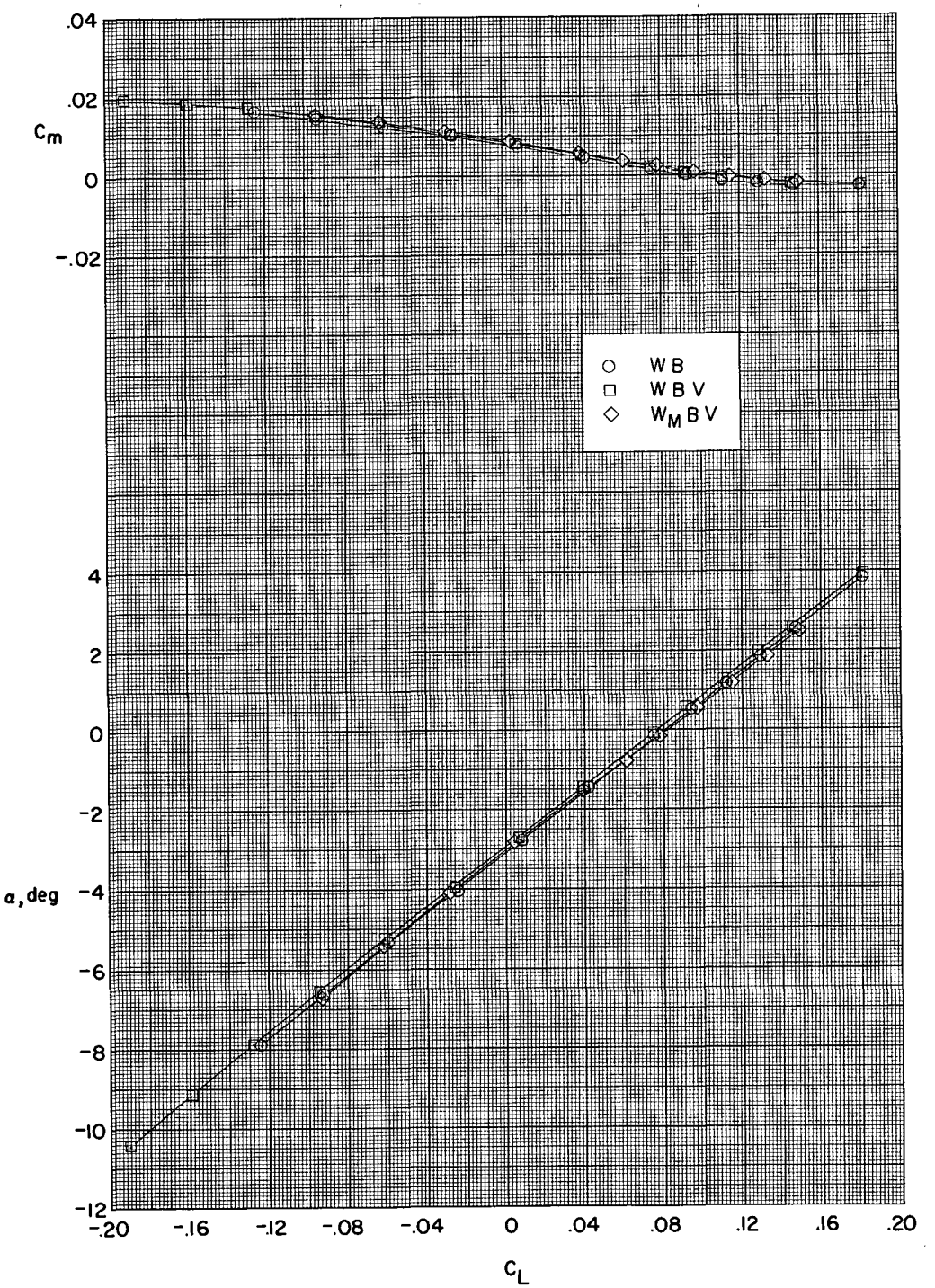


(b) M = 2.60.

Figure 8.- Continued.

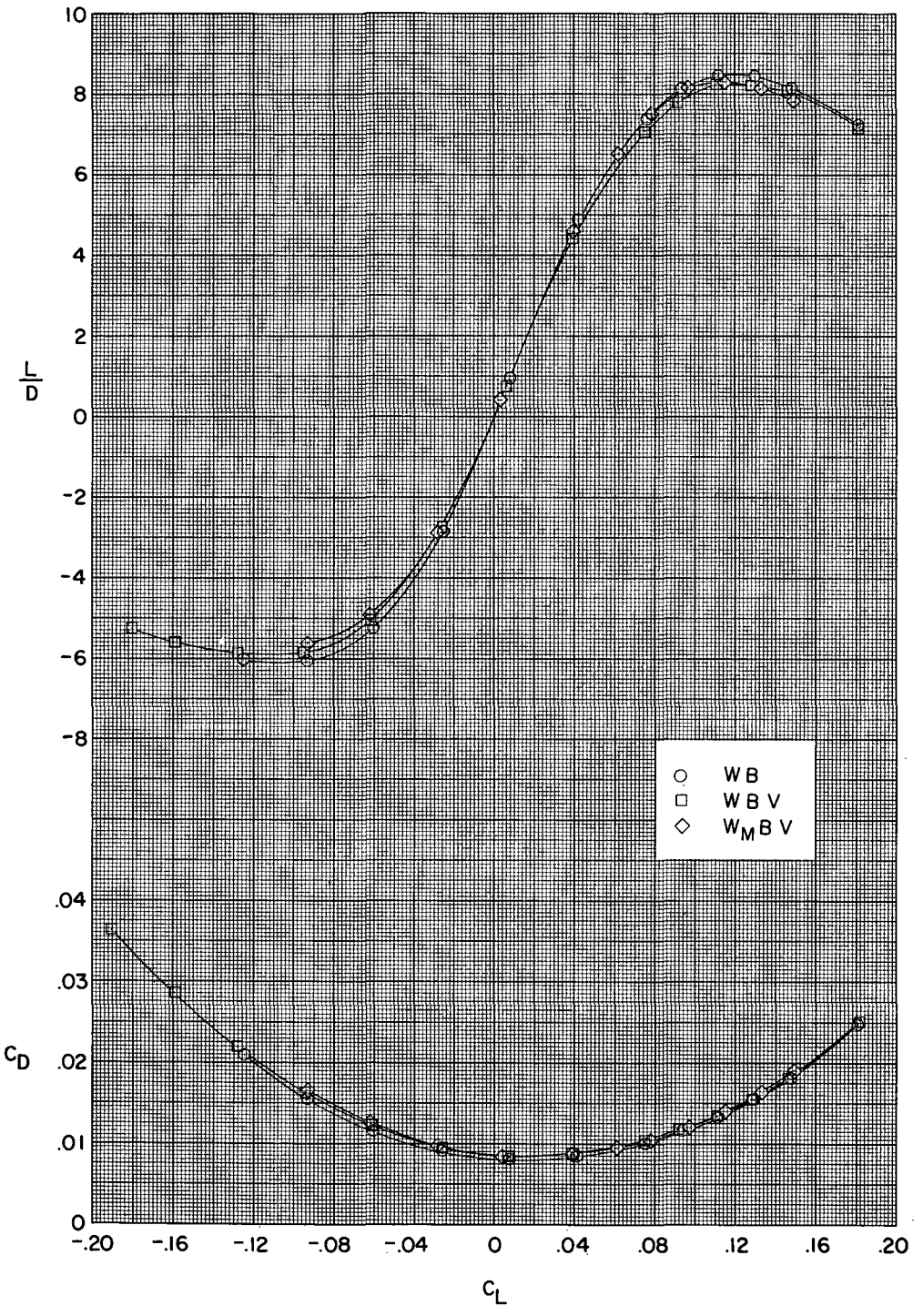


(b) Concluded.

Figure 8.- Continued.

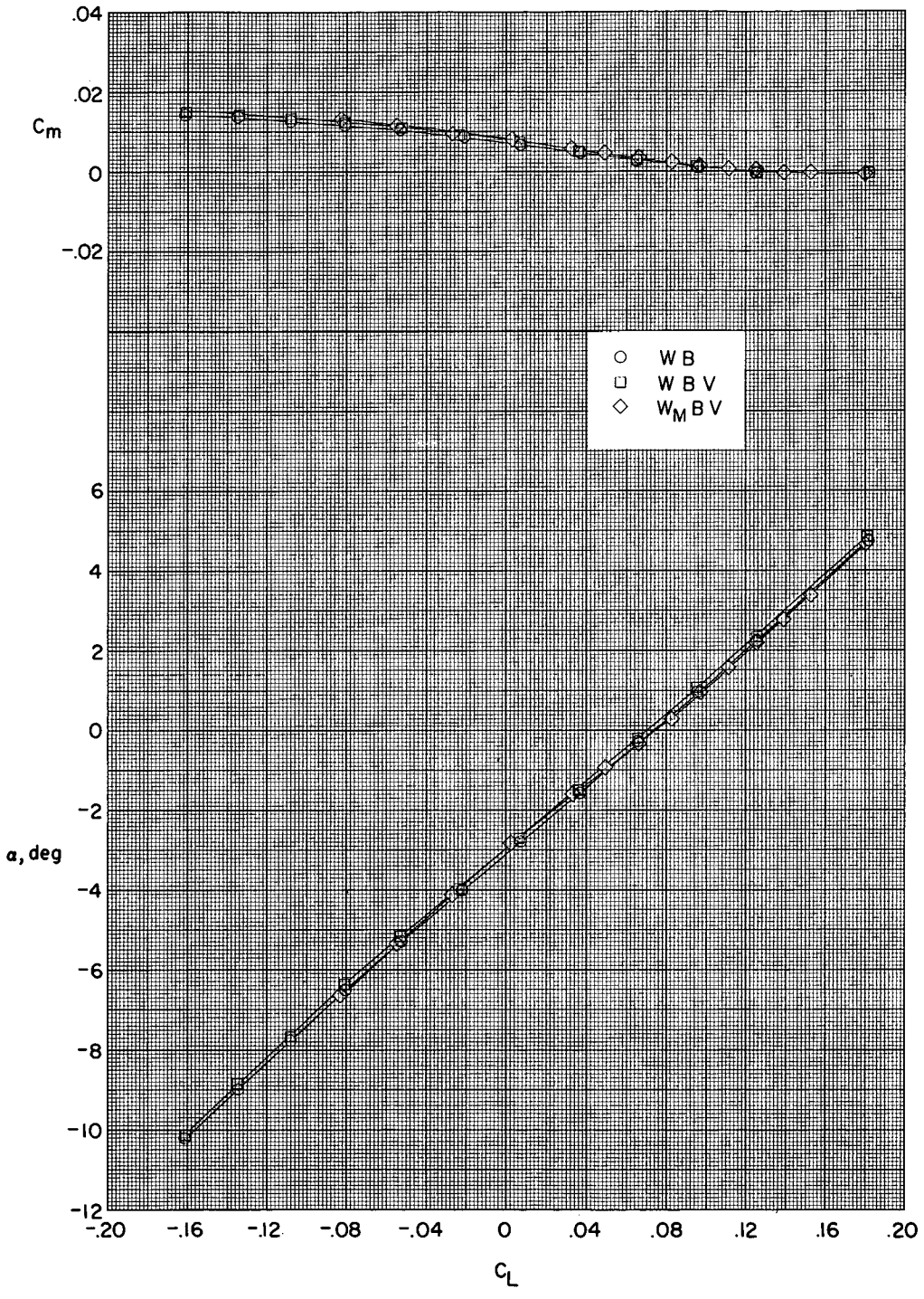


(c) M = 2.96.

Figure 8.- Continued.

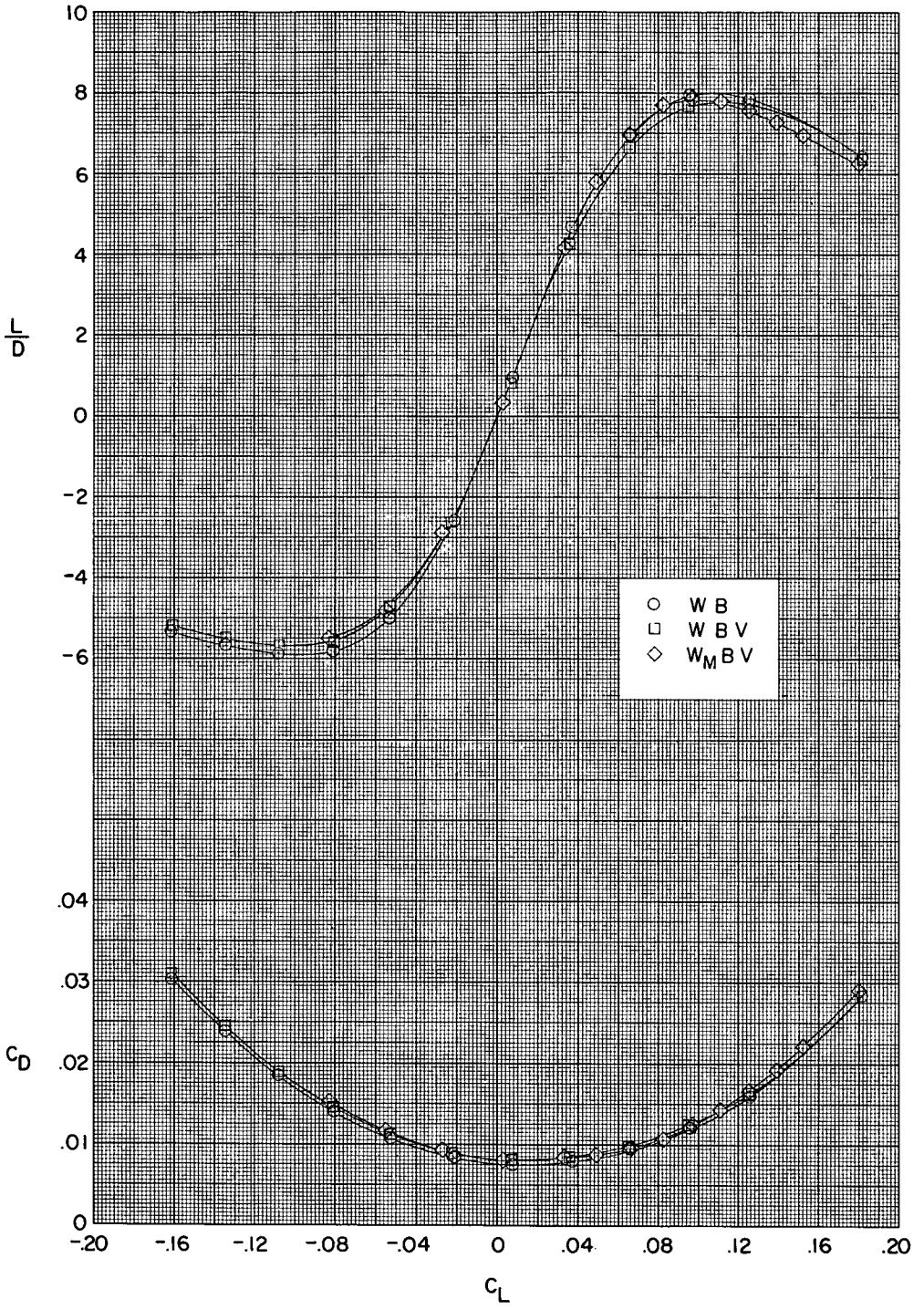


(c) Concluded.

Figure 8.- Concluded.

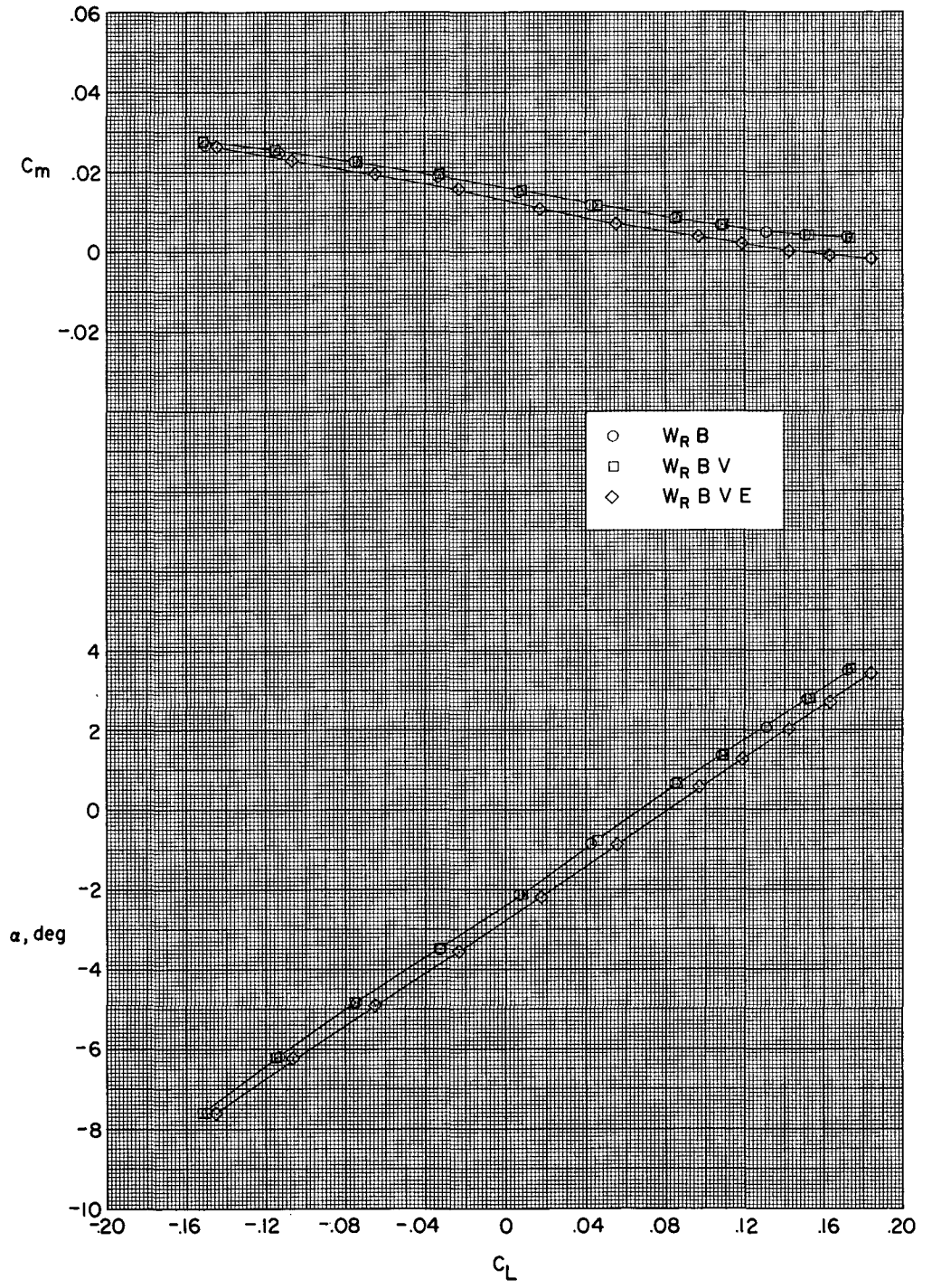


(a) M = 2.30.

Figure 9.- Effect of vertical tails and engine nacelles on longitudinal aerodynamic characteristics for reflexed-warped-wing model.

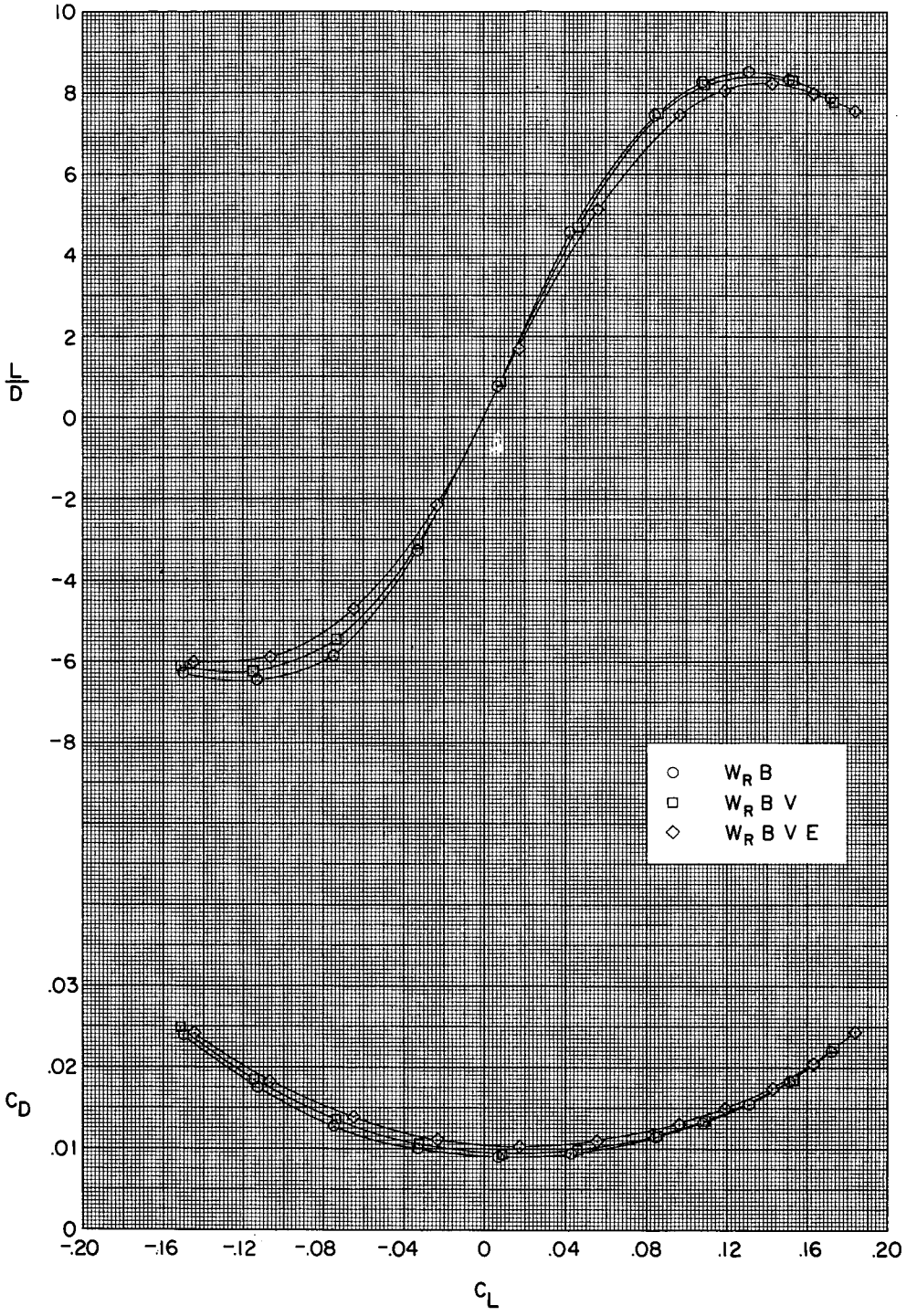


(a) Concluded.

Figure 9.- Continued.

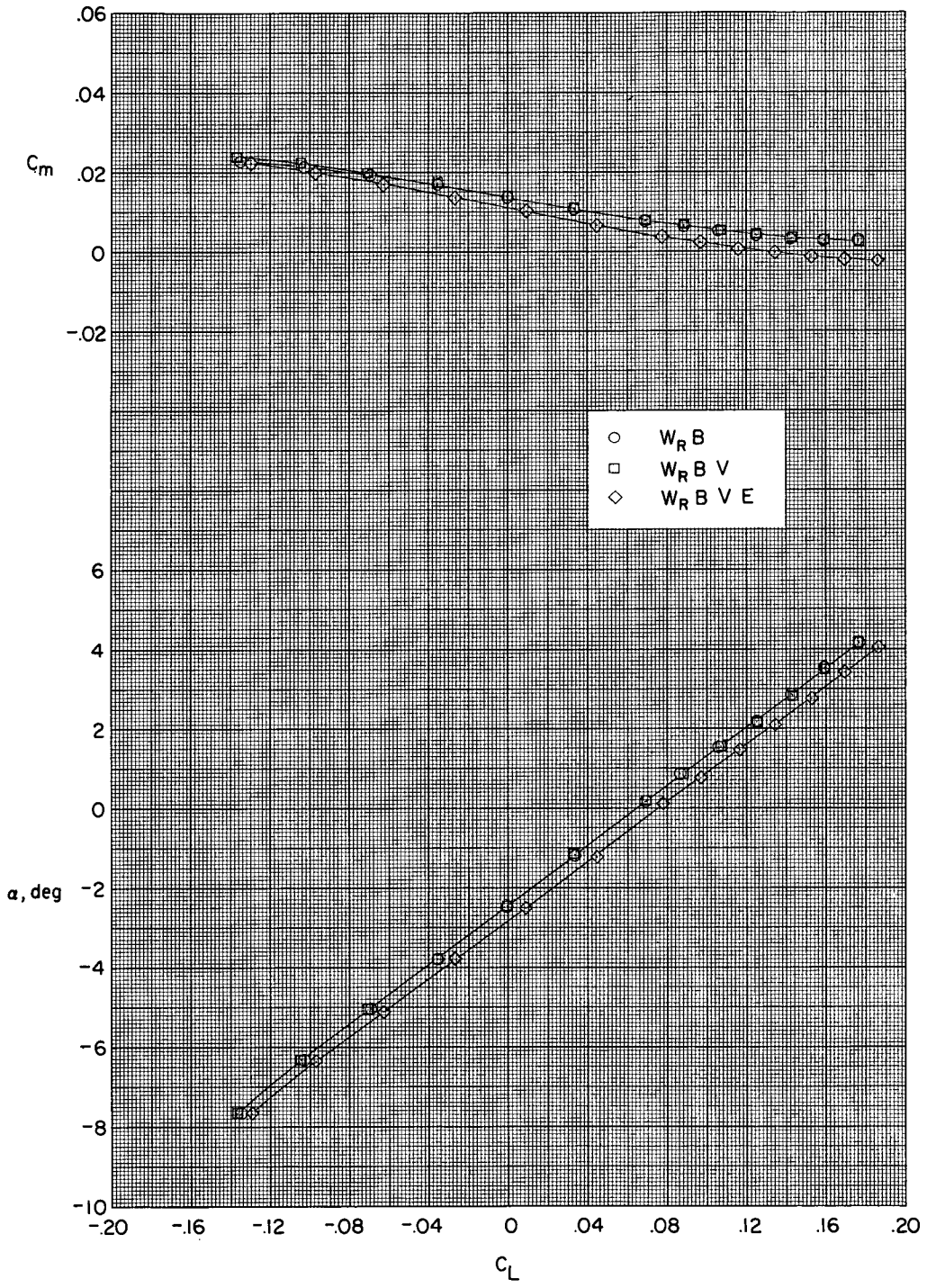


(b) M = 2.60.

Figure 9.- Continued.

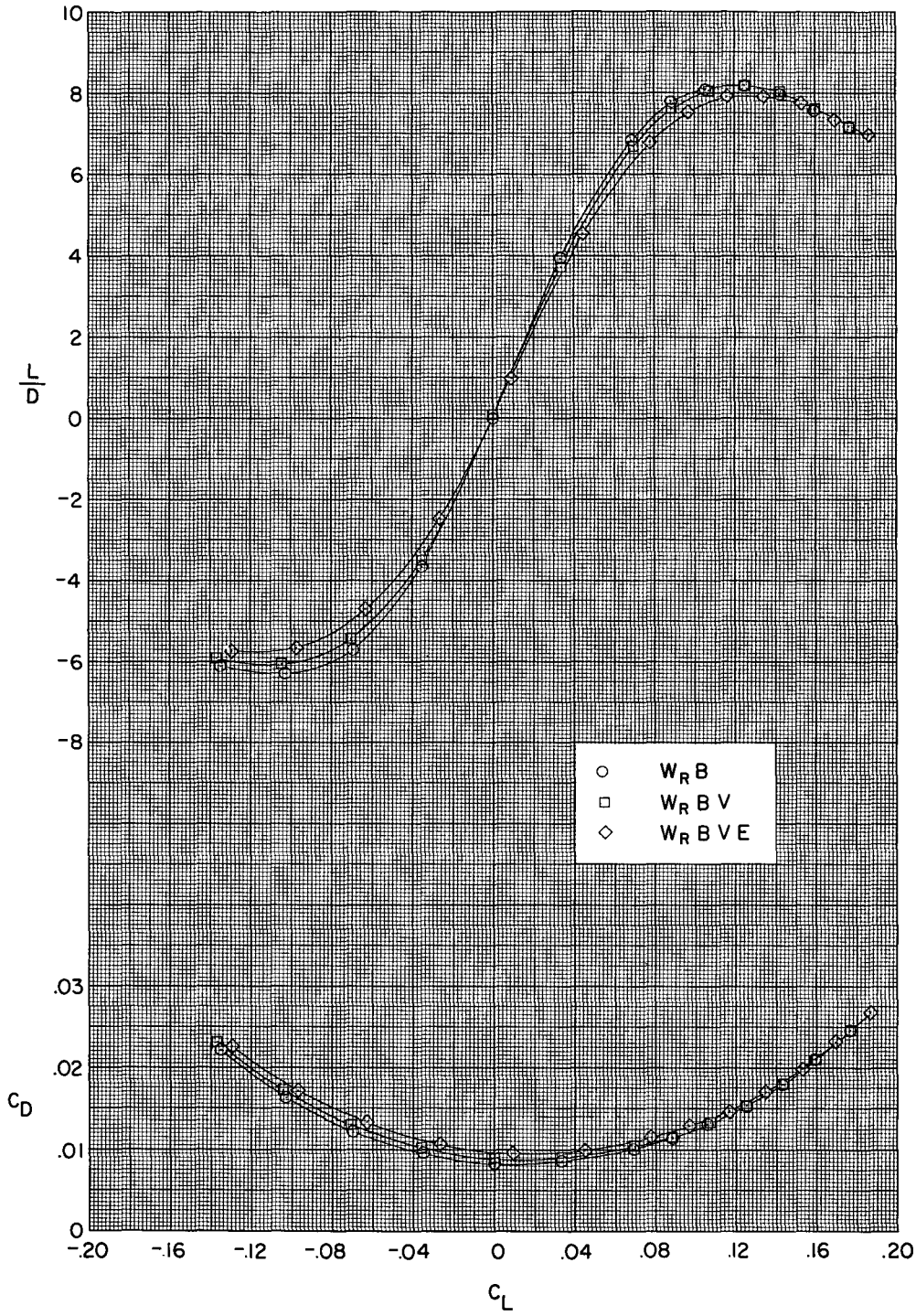


(b) Concluded.

Figure 9.- Continued.

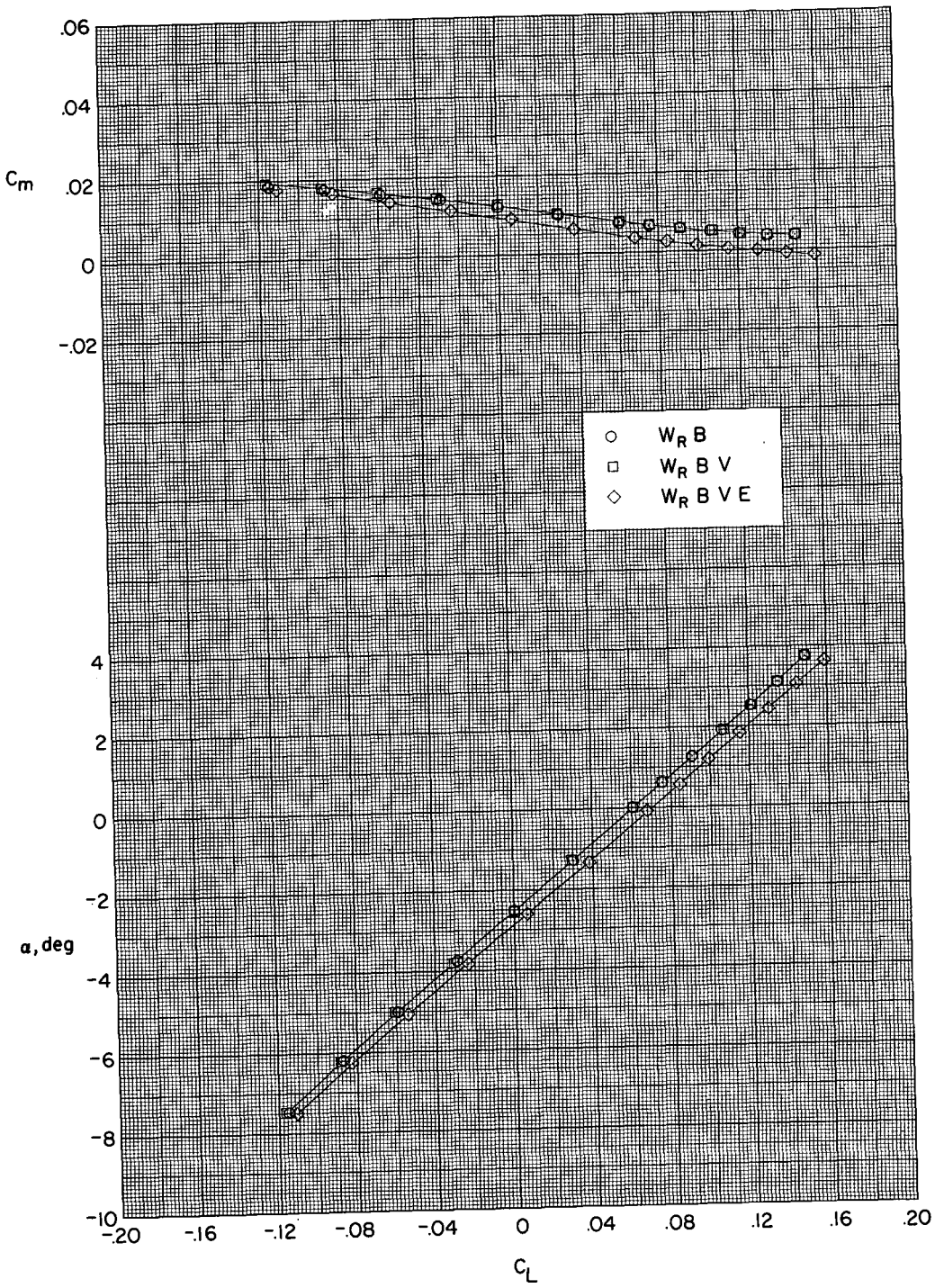


(c) M = 2.96.

Figure 9.- Continued.

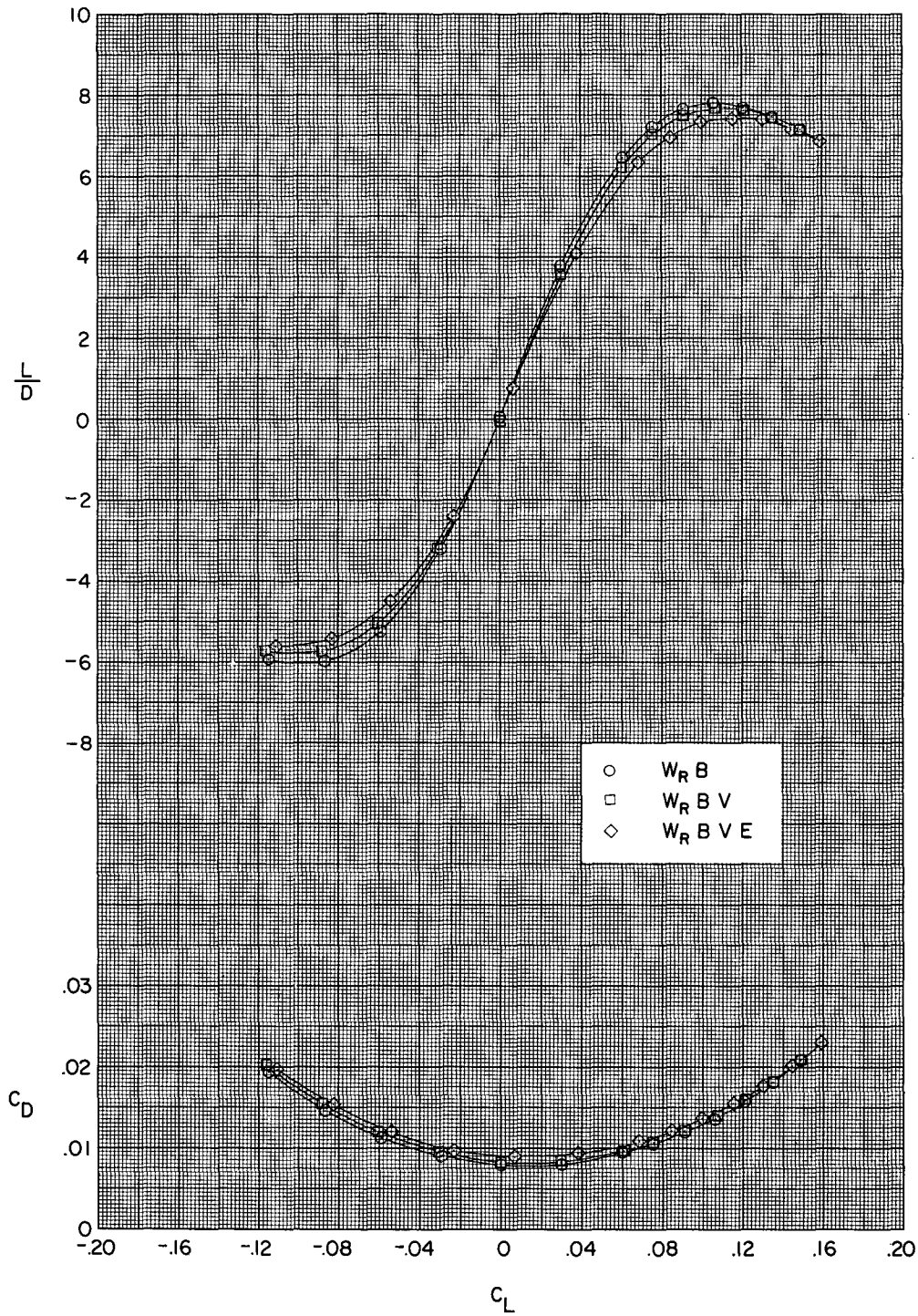


(c) Concluded.

Figure 9.- Concluded.

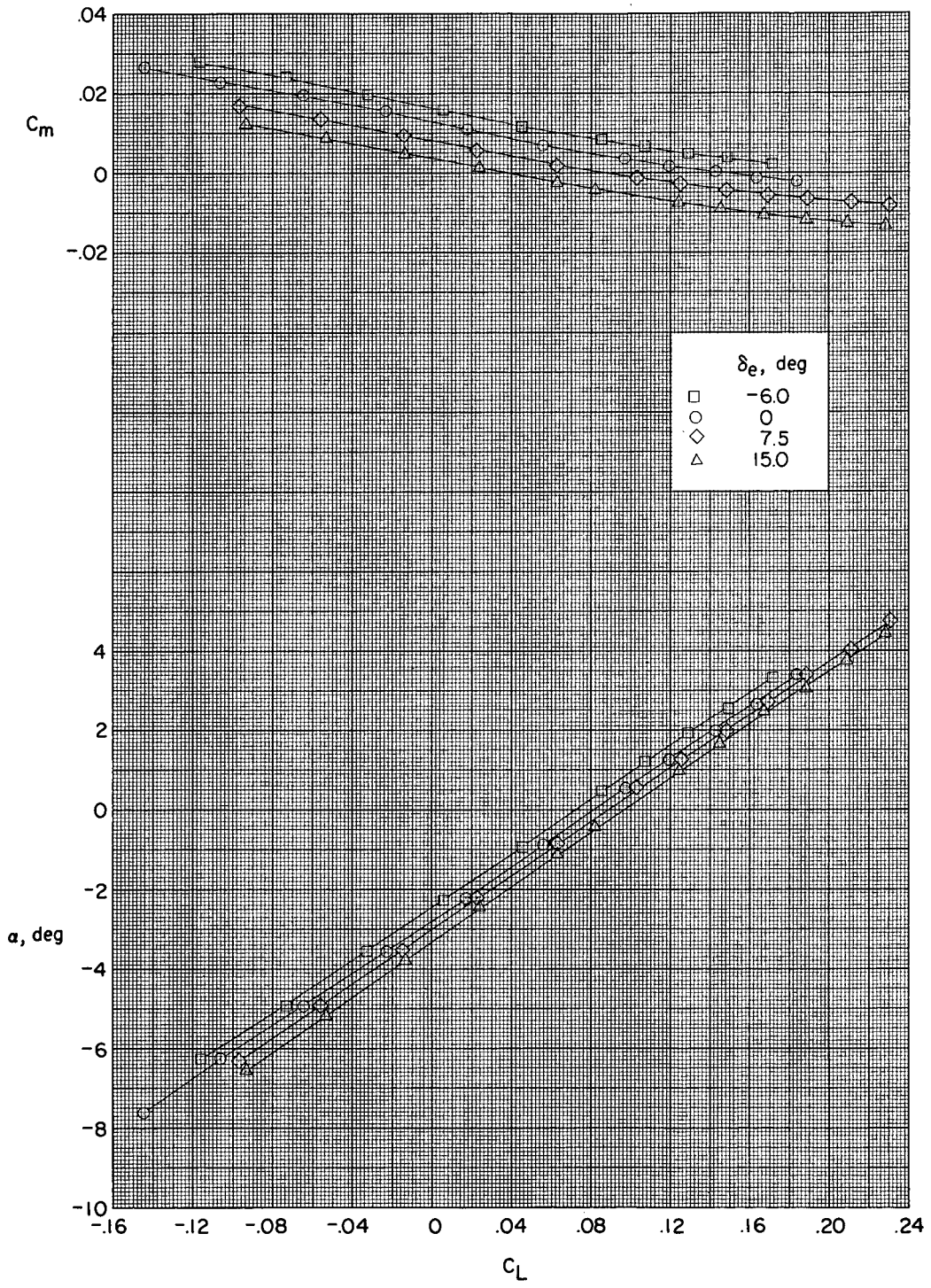


(a) M = 2.30.

Figure 10.- Effect of control deflection on longitudinal aerodynamic characteristics for complete configuration with the reflexed warped wing.

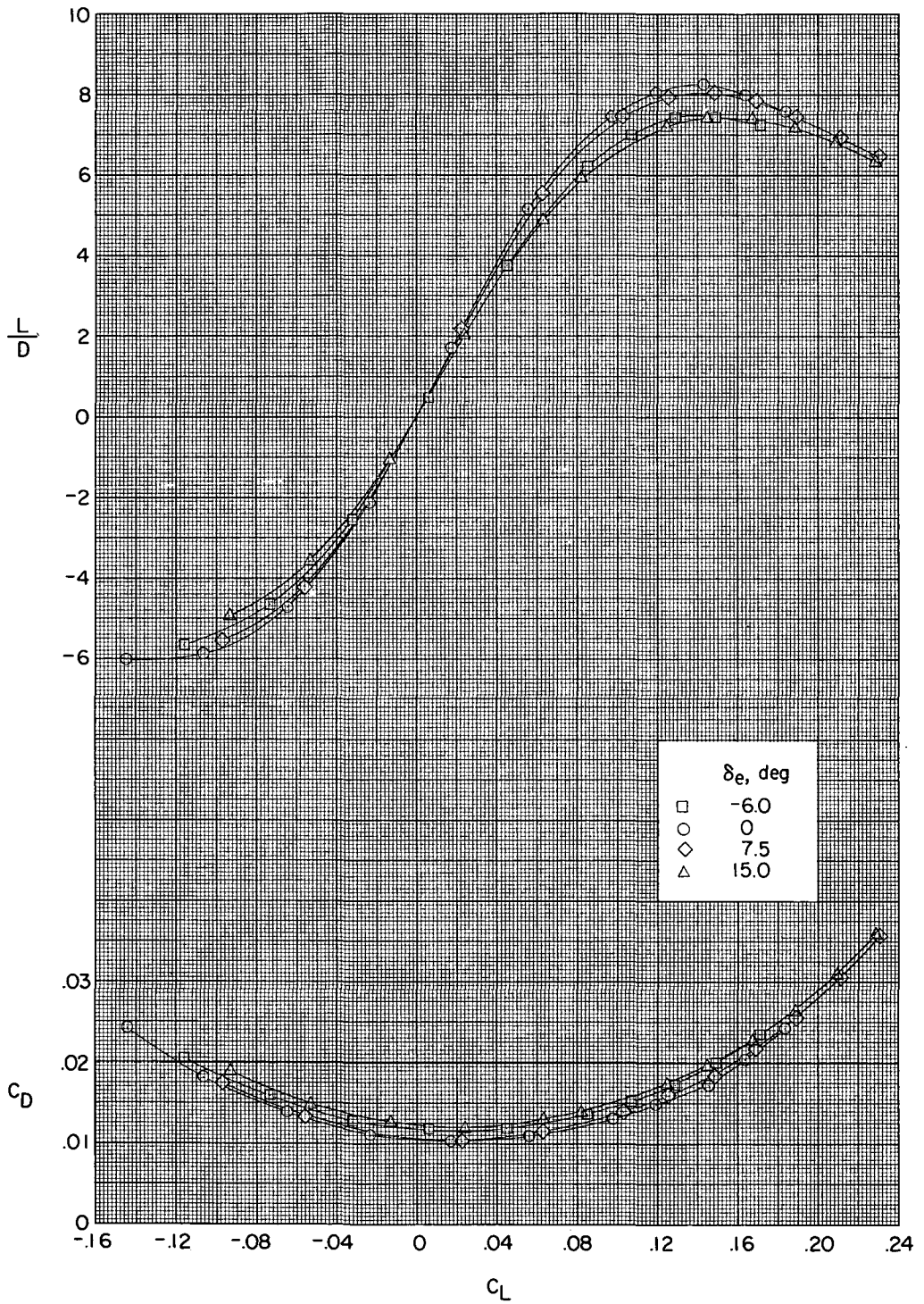


(a) Concluded.

Figure 10.- Continued.

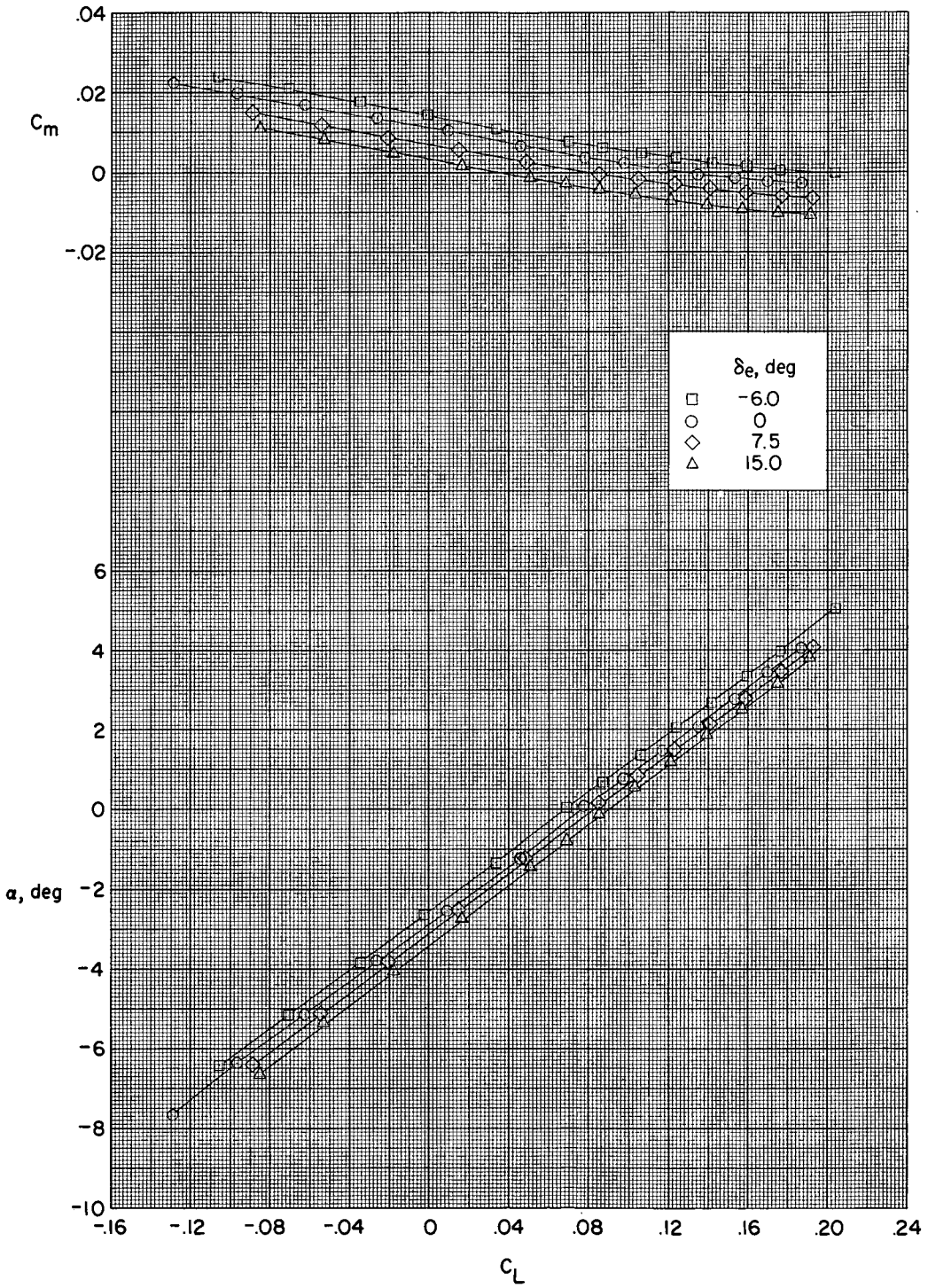


(b) M = 2.60.

Figure 10.- Continued.

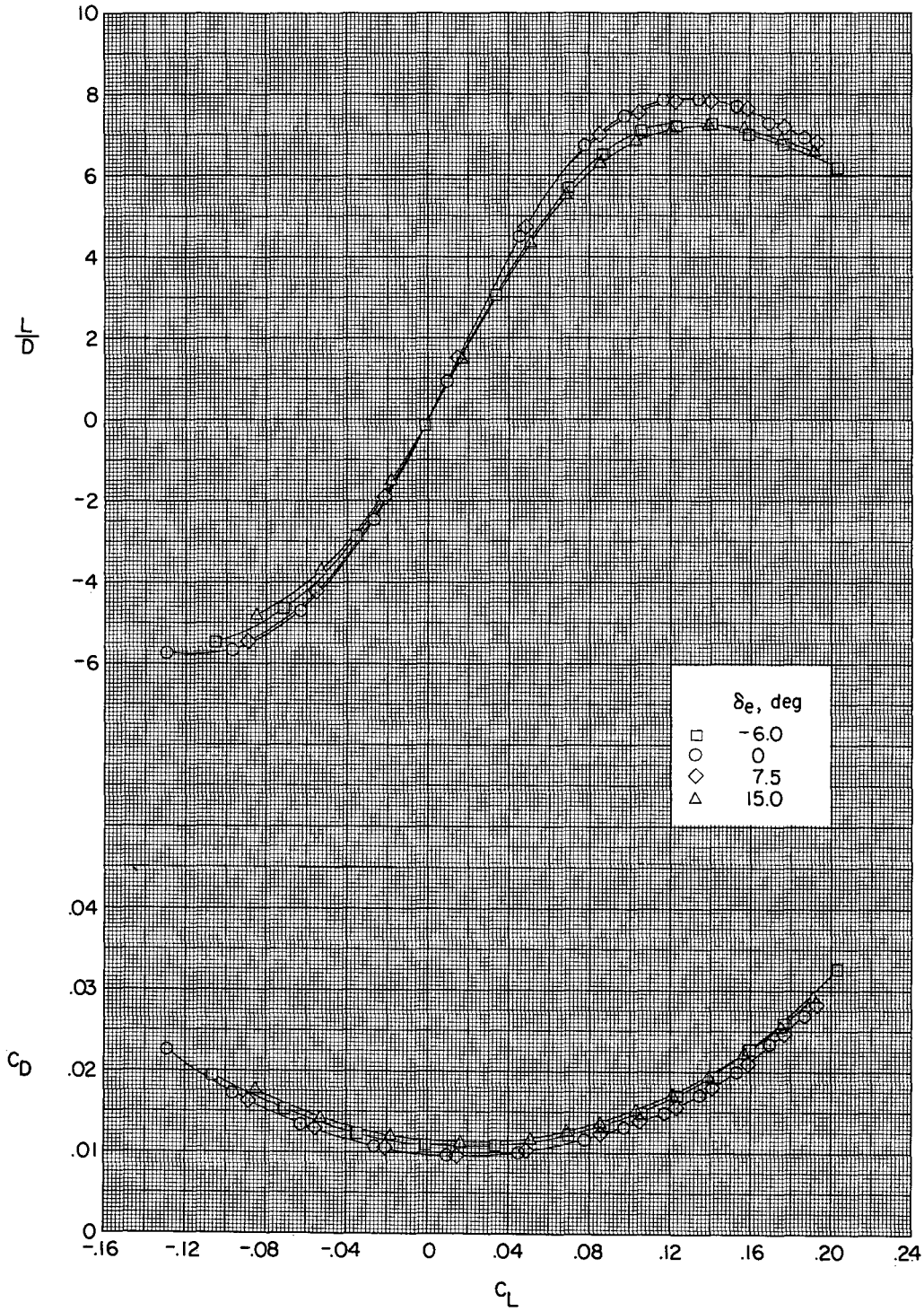


(b) Concluded.

Figure 10.- Continued.

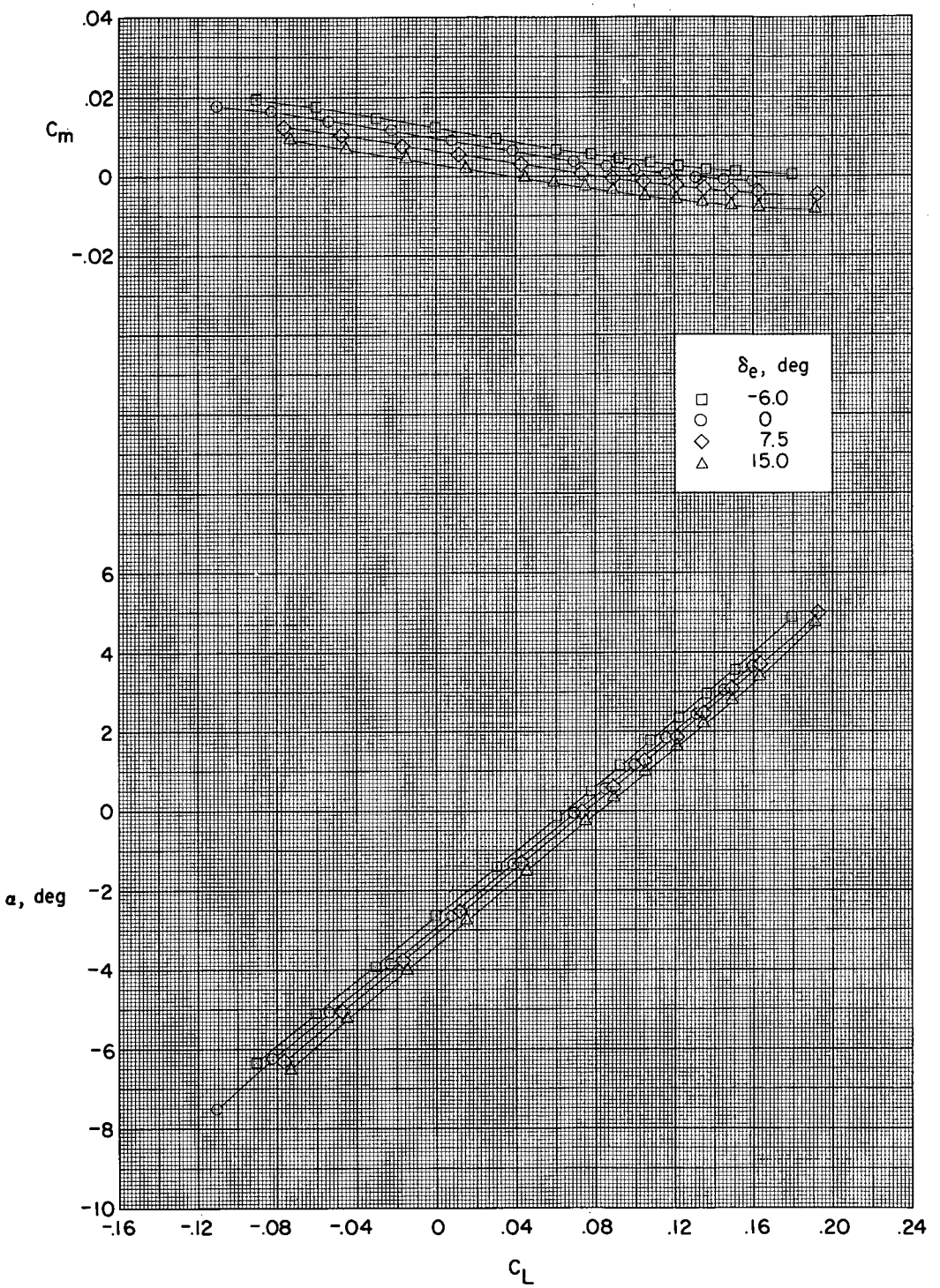


(c) M = 2.96.

Figure 10.- Continued.

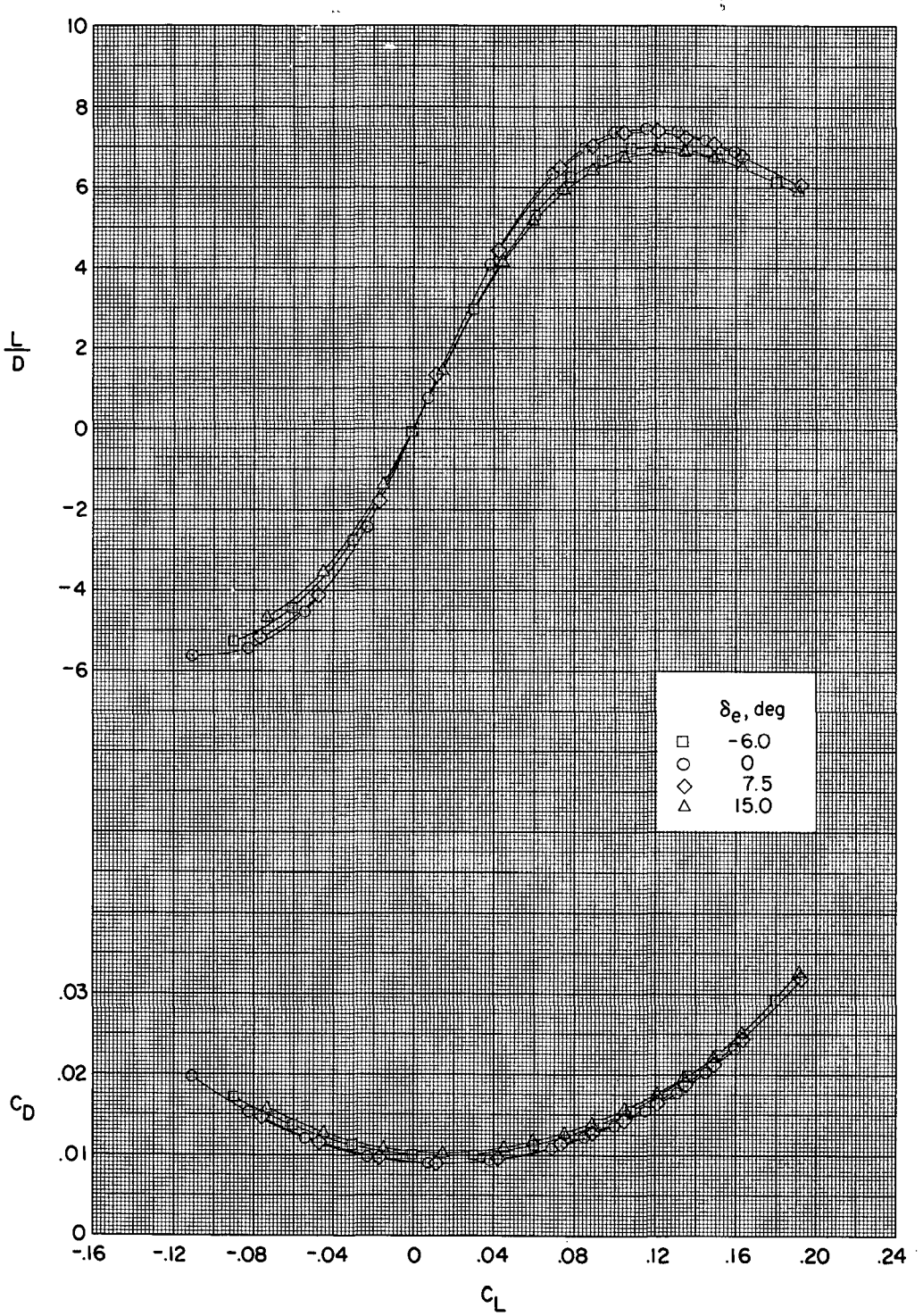


(c) Concluded.

Figure 10.- Concluded.

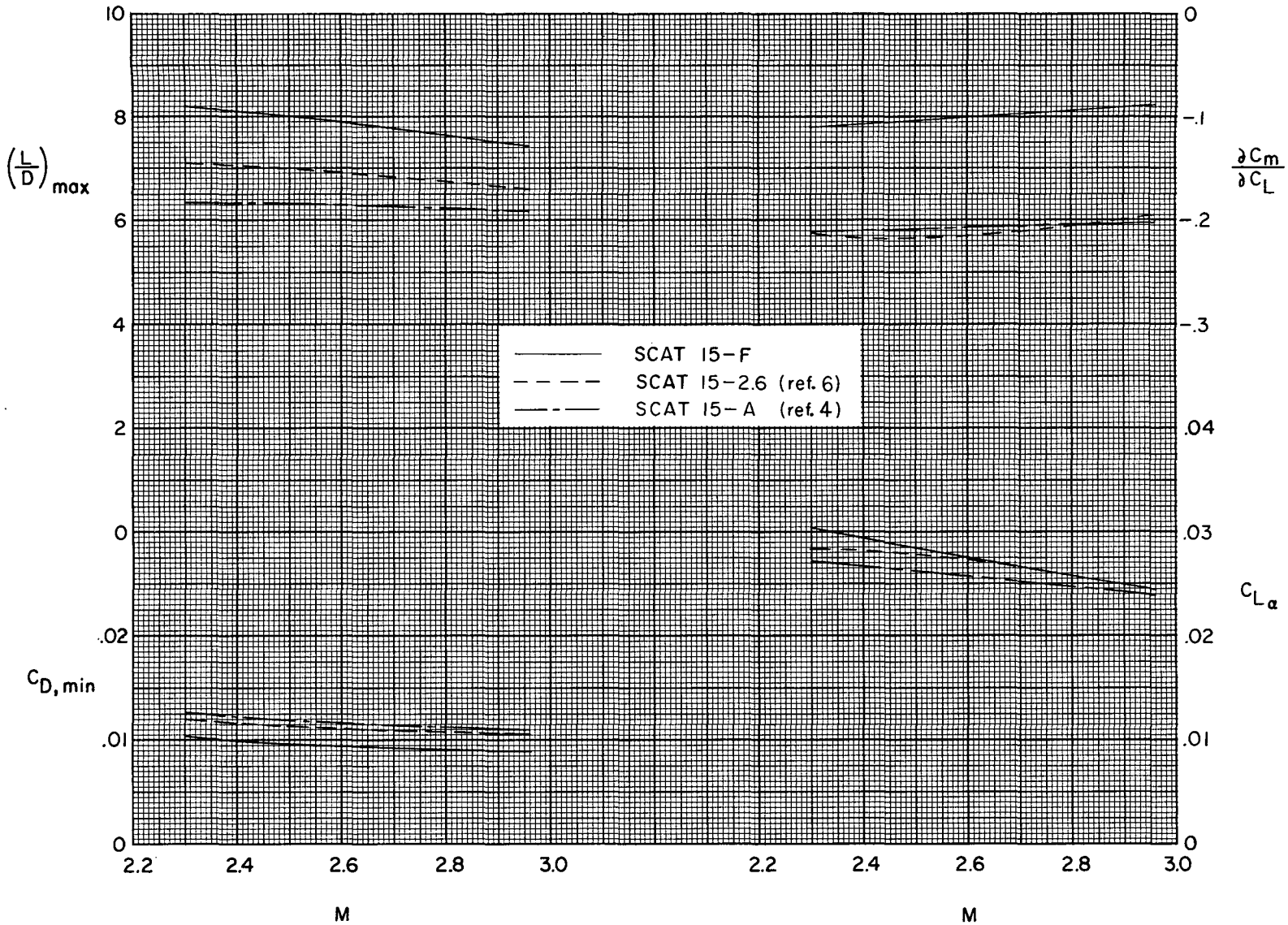


Figure 11.- Variation of longitudinal parameters with Mach number for complete configuration (SCAT 15-F) as compared with SCAT 15-A and SCAT 15-2.6.

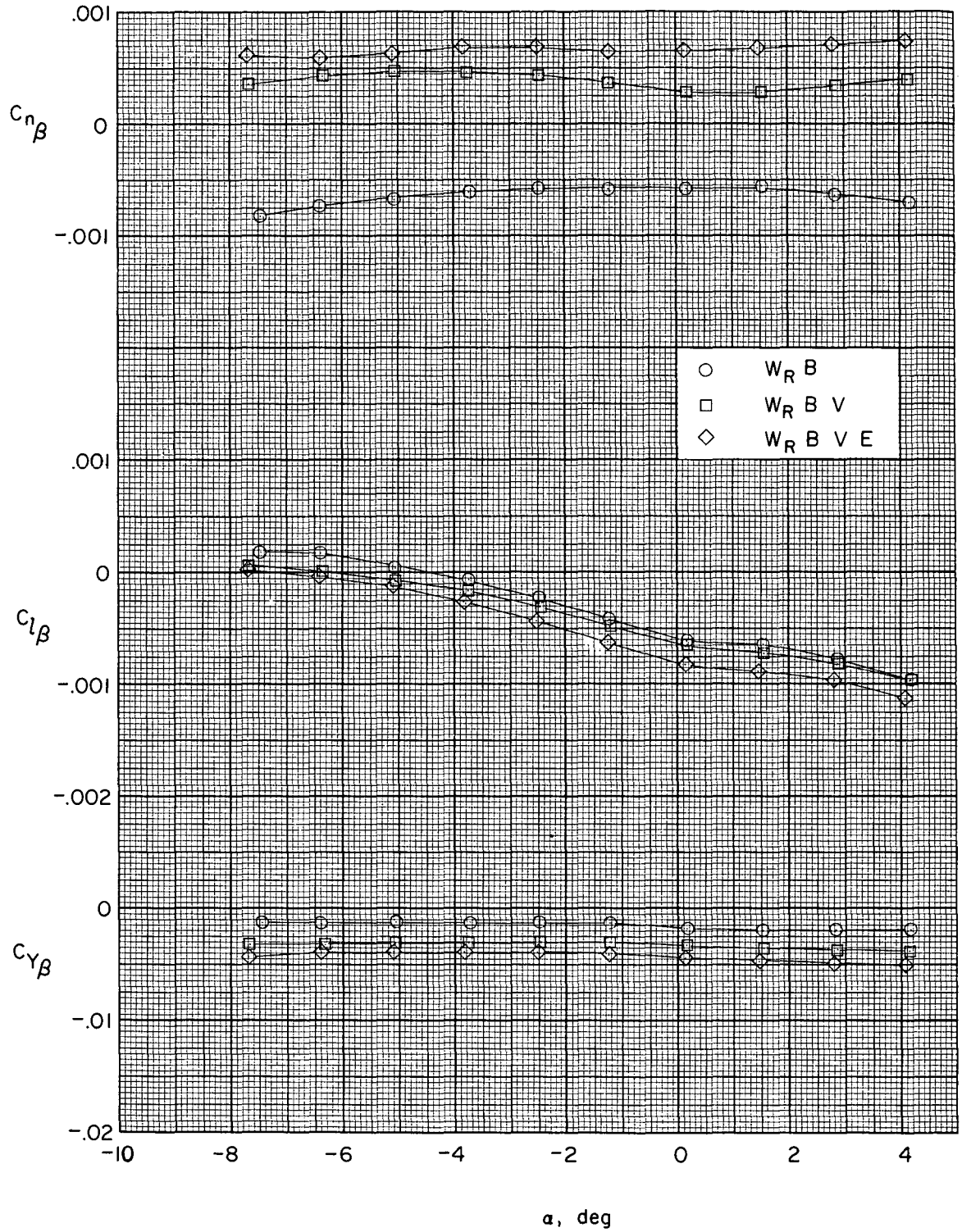


Figure 12.- Effect of vertical tails and engine nacelles on lateral aerodynamic characteristics for reflexed-warped-wing model at M = 2.60.

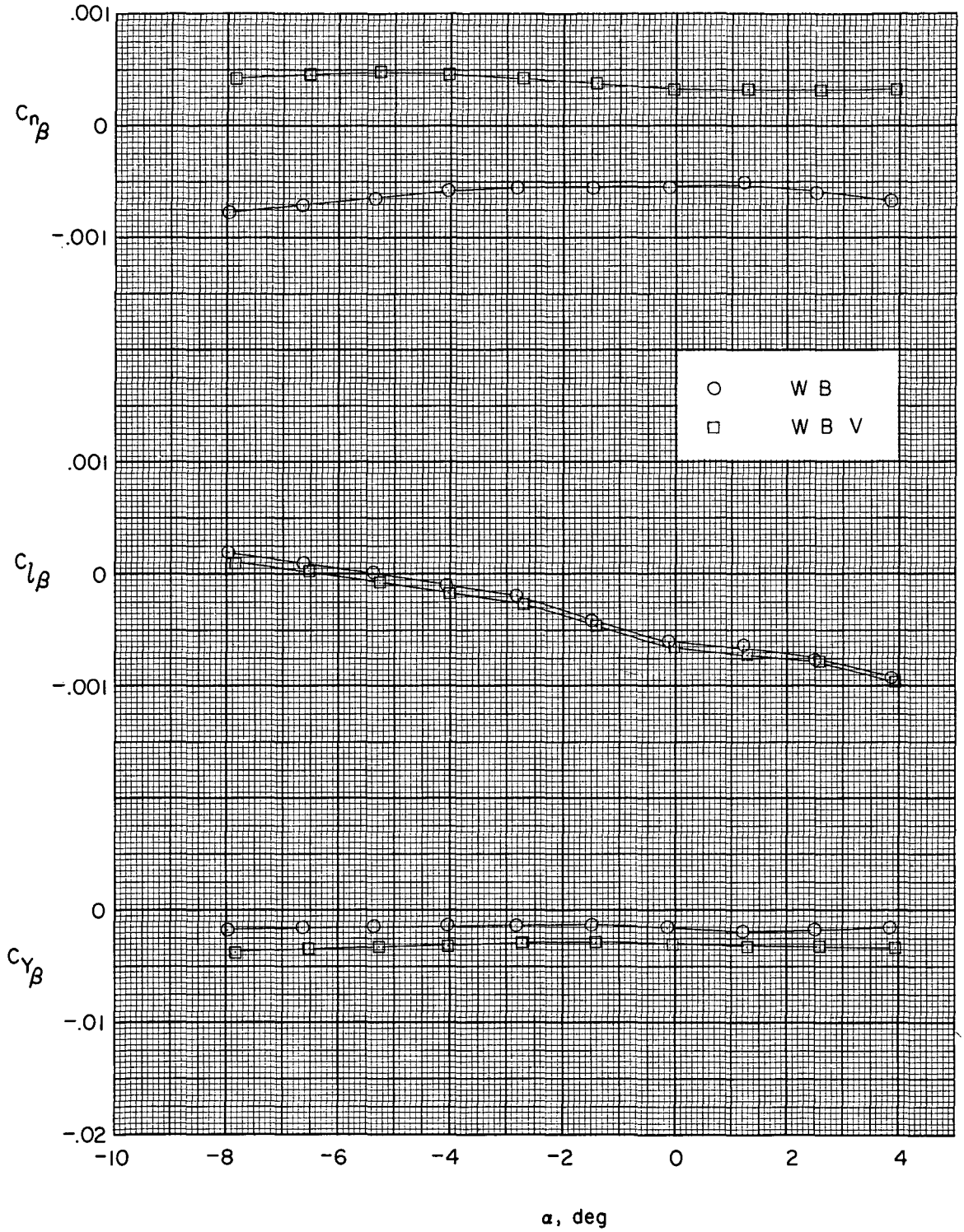


Figure 13.- Effect of vertical tails on lateral aerodynamic characteristics for unreflexed-warped-wing model at M = 2.60.